

Ch 290

ACTA POLYTECHNICA SCANDINAVICA

CHEMICAL TECHNOLOGY SERIES No. 290

**Metallocene-Catalyzed Ethene Polymerization: Long-Chain
Branched Polyethene**

ESA KOKKO

Helsinki University of Technology
Department of Chemical Technology
Laboratory of Polymer Technology
P.O.Box 6100
FIN-02015 HUT, Finland

Dissertation for the degree of Doctor of Science in Technology to be presented with due permission for public examination and debate in Auditorium Komppa at Department of Chemical Technology at Helsinki University of Technology (Espoo, Finland) on the 6th of September, 2002, at 3 o'clock afternoon.

ESPOO 2002

Kokko, Esa, **Metallocene-Catalyzed Ethene Polymerization: Long-Chain Branched Polyethene**, Acta Polytechnica Scandinavica, Chemical Technology Series No. 290, Espoo 2002, 52 pp. Published by the Finnish Academies of Technology, ISBN 951-666-602-7, ISSN 1239-0518.

Keywords: Metallocene catalysts, Polyethylene, Copolymerization, Characterization, Long-Chain Branching, Rheology

ABSTRACT

Long-chain branches and narrow molecular weight distribution is a novel structure combination in polyethene, which has only been possible to achieve with single-center catalysis. Long-chain branches, even at very low concentrations, have a strong effect on the polymer melt behavior and, thereby, the processing properties. This work deals with ethene polymerization using group IV metallocene catalysts and the examination of long-chain branching in polyethene.

Long-chain branching in metallocene catalysis is believed to take place via a copolymerization route, in which a vinyl terminated polyethene chain is incorporated into a growing polymer chain. Understanding the chain transfer mechanisms (vinyl end-group formation) and copolymerization abilities of metallocene catalysts have been important issues in this work.

The examination of the polymerization behavior of several metallocene compounds revealed that chain transfer mechanisms were catalyst specific. Depending on the catalyst structure, the termination of chain growth occurred via β -H elimination, chain transfer to the monomer, or chain transfer to the cocatalyst. The vinyl selectivities were between 20 and 100%. Comonomer response in ethene and 1-olefin copolymerization also depended on the catalyst structure. 10-fold differences in comonomer reactivity ratios were observed.

Long-chain branching analysis of homopolyethenes produced with different metallocene catalysts indicated that the catalysts with high vinyl selectivity and good copolymerization ability were the most prominent in producing a polymer with modified rheological properties. In addition to rheological measurements, ^{13}C NMR spectroscopy also showed the presence of long-chain branches. Besides the choice of catalyst, the polymerization conditions had a major impact on long-chain branch contents. Adjusting the ethene, hydrogen, or comonomer (1-olefin or nonconjugated α,ω -diene) concentration changed the rheological properties of the polymers.

© All rights reserved. No part of the publication may be reproduced, stored in a retrieval system, or transmitted in any form or by any means, electronic, mechanical, photocopying, recording, or otherwise, without the prior written permission by the author.

PREFACE

This work was carried out in the Laboratory of Polymer Technology at Helsinki University of Technology between 1997 and 2001 and in the Department of Chemical Engineering at McMaster University, Hamilton, Ontario, Canada between 2000 and 2001. The work was a part of the National Technology Agency (TEKES) research program "*New functional olefin polymers*". The financial support from TEKES and Neste Foundation is gratefully acknowledged.

I wish to express my warmest thanks to Professor Jukka Seppälä for his guidance and encouragement during this work. Also, I wish to thank Dr. Barbro Löfgren from the Polymer Science Centre for her help and cooperation.

I am most deeply indebted to my coworkers Dr. Petri Lehmus and Anneli Malmberg for the ideas and discussions we have shared. Their enthusiasm and expertise has been invaluable in this study. Many thanks to my other fellow coworkers and coauthors, Pirjo Pietikäinen and Jari Koivunen. Kimmo Hakala also deserves special thanks for maintaining and fixing our ill-behaved laboratory equipment.

I owe special thanks to Dr. Reko Leino, Dr. Hendrik Luttikhedde, and Peter Ekholm from Åbo Akademi for providing the siloxy-substituted catalysts. I am very grateful to Professor Shiping Zhu for the opportunity to carry out research work at McMaster University and to Dr. Wen-Jun Wang for the invaluable guidance with the CSTR system. I wish to thank Professor Dr. Ing. Helmut Münstedt and Dr. Ing. Claus Gabriel from the Institute of Polymeric Materials of the University of Erlangen-Nuremberg for the valuable cooperation project.

Also, I wish to acknowledge the whole personnel of the Laboratory of Polymer Technology for the good spirit shared and the wonderful times we have had during and outside of the office-hours. Also, many thanks to Ed Kolodka for all the events arranged in Hamilton.

My sincere thanks to my parents and siblings for their support and my Canadian relatives who made my stay in Hamilton a cozy one. Finally, last but not least: My deepest gratitude goes to Sanna, for her support, patience, and understanding.

Helsinki, January 8, 2002

Esa Kokko

CONTENTS

	PREFACE	
	LIST OF PUBLICATIONS	
	ABBREVIATIONS AND SYMBOLS	
1	INTRODUCTION.....	1
2	LONG-CHAIN BRANCHING IN POLYETHENE.....	4
2.1	Long-chain branching in commercial polymers.....	4
2.2	Long-chain branching mechanisms.....	4
2.3	Long-chain branching in single-center catalyzed polyethenes.....	6
2.4	Rheological properties of long-chain branched polyethenes.....	7
3	POLYMERIZATION MECHANISMS.....	10
3.1	Initiation and propagation reactions.....	10
3.2	Chain transfer reactions.....	11
3.3	Isomerization reactions.....	12
4	INFLUENCE OF POLYMERIZATION PARAMETERS ON POLYMER MICROSTRUCTURE	14
4.1	Temperature.....	14
4.2	Monomer concentration.....	15
4.2.1	The effect of ethene concentration on the vinyl selectivity and molecular weight.....	15
4.2.2	The effect of ethene concentration on the molecular weight distribution.....	17
4.3	The effect of hydrogen.....	18
4.4	Chain transfer mechanisms in examined catalysts.....	20
5	COPOLYMERIZATION OF ETHENE AND 1-OLEFINS.....	22
5.1	Influence of the ligand structure on comonomer reactivity.....	23
6	INFLUENCE OF CATALYST STRUCTURE AND POLYMERIZATION CONDITIONS ON LONG-CHAIN BRANCHING.....	26
6.1	The effect of the catalyst on branching.....	27
6.2	The effect of ethene concentration	30
6.3	The effect of hydrogen.....	33
6.4	The effect of comonomer	33
7	CORRELATION OF RHEOLOGICAL PROPERTIES WITH POLYMER STRUCTURE.....	36
7.1	Correlation between the analytical methods.....	41
8	SUMMARY.....	42
	REFERENCES.....	43
	APPENDICES, PAPERS I-VIII	

LIST OF PUBLICATIONS

- I Malmberg, A., Kokko, E., Lehmus, P., Löfgren, B., Seppälä, J.V., Long-Chain Branched Polyethene Polymerized by Metallocene Catalysts Et[Ind]₂ZrCl₂/MAO and Et[IndH₄]₂ZrCl₂/MAO, *Macromolecules* **31** (1998) 8448-8454.
- II Lehmus, P., Kokko, E., Härkki, O., Leino, R., Luttikhedde, H.J.G., Näsman, J.H., Seppälä, J.V., Homo- and Copolymerization of Ethylene and alpha-Olefins over 1- and 2-Siloxy-Substituted Ethylenebis(indenyl)zirconium and Ethylenebis(tetrahydroindenyl)-zirconium Dichlorides, *Macromolecules* **32** (1999) 3547-3552.
- III Kokko, E., Malmberg, A., Lehmus, P., Löfgren, B., Seppälä, J. Influence of the Catalyst and Polymerization Conditions on the Long-Chain Branching of Metallocene-Catalyzed Polyethenes, *J. Polym. Sci. Part A: Polym. Chem.* **38** (2000) 376-388.
- IV Kokko, E., Lehmus, P., Leino, R., Luttikhedde, H.J.G., Ekholm, P., Näsman, J.H., Seppälä, J.V. meso- and rac-Diastereomers of 1- and 2-tert-Butyldimethylsiloxy Substituted Ethylenebis(indenyl)zirconium Dichlorides for Formation of Short- and Long-Chain Branched Polyethene, *Macromolecules* **33** (2000) 9200-9204.
- V Kokko, E., Lehmus, P., Malmberg, A., Löfgren, B., Seppälä, J., Long-Chain Branched Polyethene via Metallocene-Catalysis: Comparison of Catalysts. In *Organometallic Catalyst and Olefin Polymerization, Catalysts for a New Millennium*, Blom, R., Follestad, A., Rytter, E., Tilset, M., Ystenes, M (Eds.) Springer, 2001, 335-345.
- VI Kokko, E., Pietikäinen, P., Koivunen, J., Seppälä, J.V., Long-Chain-Branched Polyethene by the Copolymerization of Ethene and Nonconjugated α,ω -Dienes. *J. Polym. Sci. Part A: Polym. Chem.* **39** (2001) 3805-3817.
- VII Kokko, E., Wang, W.-J., Zhu, S., Seppälä, J.V., Structural Analysis of Polyethene Prepared with rac-Dimethylsilylbis(indenyl)zirconium Dichloride/Methylaluminumoxane in High-Temperature Continuous Stirred-Tank Reactor, *J. Polym. Sci. Part A: Polym. Chem.* **40** (2002) 3292-3301.
- VIII Gabriel, C., Kokko, E., Löfgren, B., Seppälä, J.V., Münstedt, H., Analytical and Rheological Characterization of Long-Chain Branched Metallocene-Catalyzed Ethylene-Homopolymers, *Polymer* **43** (2002), in press.

The author's contribution to the appended publications:

- I** The author participated in the experimental planning, and carried out half of the experimental work and half of the preparation of the manuscript.
- II** The author participated in the experimental planning, experimental work, and assisted in the preparation of the manuscript.
- III** The author planned the experiments, carried out the major part of the experimental work, and prepared the manuscript with the coauthors.
- IV** The author planned and carried out the polymerization experiments, polymer characterization, and prepared the manuscript with the coauthors.
- V** The author planned and carried out the polymerizations, polymer characterization work, and prepared the manuscript with the assistance of the coauthors.
- VI** The author planned and guided the polymerization experiments with the second author, carried out the rheological characterization work, and wrote the paper with the assistance of the coauthors.
- VII** The author planned and carried out the polymerizations, polymer characterization, and prepared the manuscript with the assistance of the coauthors.
- VIII** The author carried out the polymerizations, part of the characterization work, and wrote the corresponding part of the paper.

ABBREVIATIONS AND SYMBOLS

Bu	butyl
CGC	constrained geometry catalyst, $[\text{CpMe}_4\text{SiMe}_2\text{N}(\text{t-Bu})]\text{TiCl}_2$
CSTR	continuous stirred-tank reactor
Cp	cyclopentadienyl
DSC	differential scanning calorimetry
Et	ethyl
Flu	fluorenyl
FTIR	fourier transform infrared
GPC	gel permeation chromatography
H ₄ Ind	tetrahydroindenyl
HD	hexadiene
Ind	indenyl
<i>i</i> Pr	isopropyl
LCB	long-chain branch
M	transition metal (Ti, Zr, or Hf)
MAO	methylaluminoxane
Me	methyl
NMR	nuclear magnetic resonance
OD	octadiene
PE-HD	high-density polyethene
PE-LD	low-density polyethene
PE-LLD	linear low-density polyethene
Ph	phenyl
rac	racemic
SCB	short-chain branch

Symbols

$[\text{C}^*]$	active-site concentration	mol/L
$[\text{C}_2\text{H}_4]$	ethene concentration	mol/L
$[\text{M}]$	monomer concentration	mol/L
ε	molar coefficient factor	1/mm
ϕ	volume fraction	-
Λ	activation coefficient	kJ/mol
η^*	complex viscosity	$\text{Pa}\times\text{s}$
η_0	zero-shear viscosity	$\text{Pa}\times\text{s}$
η_E	elongational viscosity	$\text{Pa}\times\text{s}$
A	absorption	-
b	film thickness	mm
C_E	ethene concentration	mol/L
E_a	flow activation energy	kJ/mol
$E_{a,0}$	flow activation energy at zero shear rate	kJ/mol
$E_{a,L}$	flow activation energy of linear polymer	kJ/mol
$E_{a,B}$	flow activation energy of branched polymer	kJ/mol
G'	storage modulus	Pa
G''	loss modulus	Pa

$g(M)$	contraction factor	-
k	rate constant, see subscripts	unit depends on the equation
M_A	molecular weight of the arm (equal to M_w)	g/mol
M_c	critical molecular weight	g/mol
M_E	entanglement molecular weight	g/mol
M_n	number average molecular weight	g/mol
M_w	weight average molecular weight	g/mol
M_w/M_n	molecular weight distribution, molar mass distribution	-
R	reaction rate, see subscripts	unit depends on the equation
R^2	correlation coefficient	-
r	reactivity ratio	-
X_n	number average polymerization degree	-

Subscripts

p	propagation
tr, M	chain transfer to monomer
$tr, \beta\text{-H}$	β -H elimination
tr, H_2	chain transfer to hydrogen
tr, Al	chain transfer to aluminum
tr, σ	chain transfer to monomer via σ -bond metathesis

1 INTRODUCTION

Polyethylene is the most widely used synthetic polymer material and its use accounts for one third of the total plastics market. The commercial production of polyethylene was 52 Mtons in 2000, and the annual growth rate for the next five years has been estimated to be 6 % [1]. In addition to the overall increase in demand due to economic growth, a key factor in the increased consumption of polyethylene products has been the continuing improvement in polyethylene properties and polymerization processes.

The properties of polyethylene are strongly influenced by its molecular weight, molecular weight distribution (M_w/M_n), and branching. The effect of branching on the properties of polyethylene depends on the length and the amount of the branches. Short-chain branches (SCB), of less than approximately 40 carbon atoms, interfere with the formation of the crystal structure. Short branches mainly influence the mechanical and thermal properties. As the branch length increases, they are able to form lamellar crystals of their own and the influence on the mechanical and thermal properties is diminished. Long branches – whose length is longer than the average critical entanglement distance of a linear polymer chain – have a tremendous effect on the melt rheological behavior. Even very small quantities of long-chain branching (LCB) alter the polymer processing properties significantly.

Conventional high-pressure low-density polyethylene (PE-LD) grades have a broad M_w/M_n and the polymers contain some LCB. This structure makes PE-LD easy to process. However, the broad M_w/M_n causes the mechanical properties of PE-LD to be inferior to those of linear low-density polyethylene (PE-LLD), which has a narrower M_w/M_n .

Highly active metallocene catalysts for the polymerization of olefins [2-6] have enabled the production of linear, narrow M_w/M_n polyethenes with greatly improved mechanical properties. The processability of these polymers, however, is more difficult when compared to the grades with the broad M_w/M_n and LCB. The introduction of LCB in the metallocene-catalyzed polyethenes can help to improve the poor processability. The combination of the good mechanical properties of metallocene-catalyzed polyethenes with the good processability of PE-LD is an obvious target.

This thesis has four objectives. The first is to show evidence of LCB in polymer materials of this investigation. The evidence of LCB in polymer materials is based on

^{13}C NMR spectroscopy and rheological measurements [I]. This is discussed in Chapter 2. In addition, a general discussion of LCB in polyethene is provided.

The second objective is to study the polymerization behavior of a limited number of metallocene/methylaluminoxane catalyst systems. The role of the catalyst is of interest because not all metallocenes are capable of producing LCB polyethene. Figure 1.1 shows the metallocene complexes chosen for this study. These catalysts were expected to produce polyethene with similar molecular weights and polymerization activity but still have significant differences in their polymerization behavior. This part focuses on examining the vinyl end group selectivity (chain transfer mechanisms) and copolymerization ability. Polymerization mechanisms and the influence of polymerization parameters on polymer structure are discussed in Chapters 3 and 4. The copolymerization abilities of the catalysts are discussed in Chapter 5 [II-V].

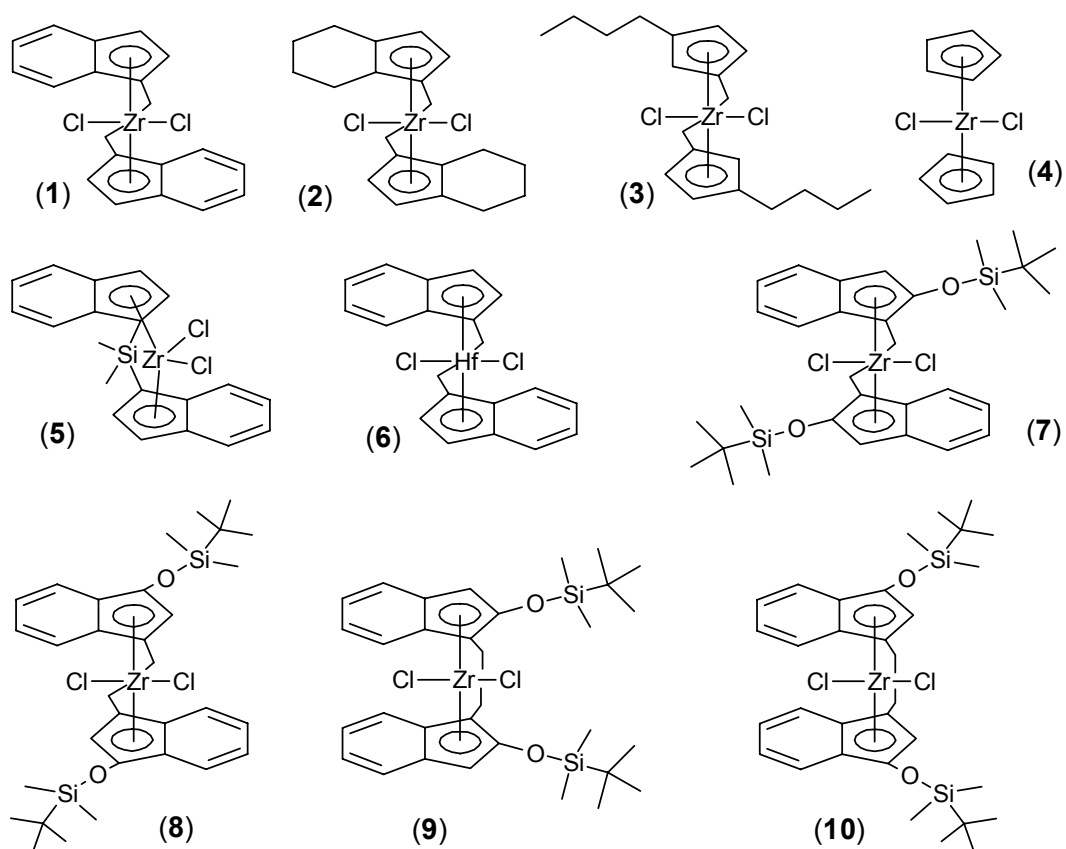


Figure 1.1 Catalyst precursors used in this study: (1) *rac*-Et[Ind]₂ZrCl₂; (2) *rac*-Et[H₄Ind]₂ZrCl₂; (3) (*n*-BuCp)₂ZrCl₂; (4) Cp₂ZrCl₂; (5) *rac*-Me₂Si[Ind]₂ZrCl₂; (6) *rac*-Et[Ind]₂HfCl₂; (7) *rac*-Et[2-*tert*-BuSiMe₂OInd]₂ZrCl₂; (8) *rac*-Et[3-*tert*-BuSiMe₂OInd]₂ZrCl₂; (9) *meso*-Et[2-*tert*-BuSiMe₂OInd]₂ZrCl₂; (10) *meso*-Et[3-*tert*-BuSiMe₂OInd]₂ZrCl₂.

The third aim is to evaluate the influence of catalyst structure and polymerization conditions on LCB as they are likely to have a great impact on LCB density. Chapter 6 includes this discussion. A comparison is made between the observed melt rheological behavior of the polyethenes and the employed catalyst systems in order to find a correlation between the catalyst and LCB [I, III, V]. Also, the influence of the process parameters – ethene concentration and polymerization time – on the reactivity of macromonomers as well as the parameters affecting the vinyl end group selectivity – hydrogen, comonomer, and diene concentration – are studied with the selected catalysts [III, V, VI]. In addition, the properties of polyethene obtained in solution polymerization are studied. [VII]

The fourth part of the thesis, Chapter 7, deals with the comparison of different analytical methods in detecting LCB and the correlation between polymer structure and polymer melt behavior [VII, VIII].

2 LONG-CHAIN BRANCHING IN POLYETHENE

2.1 Long-chain branching in commercial polymers

Long-chain branching in conventional PE-LD has been studied thoroughly. [7] The source of LCB in free-radical polymerization at high temperatures and pressures is the intermolecular chain transfer. Short-chain branching in PE-LD results from intramolecular chain transfer [8, pp. 395-400].

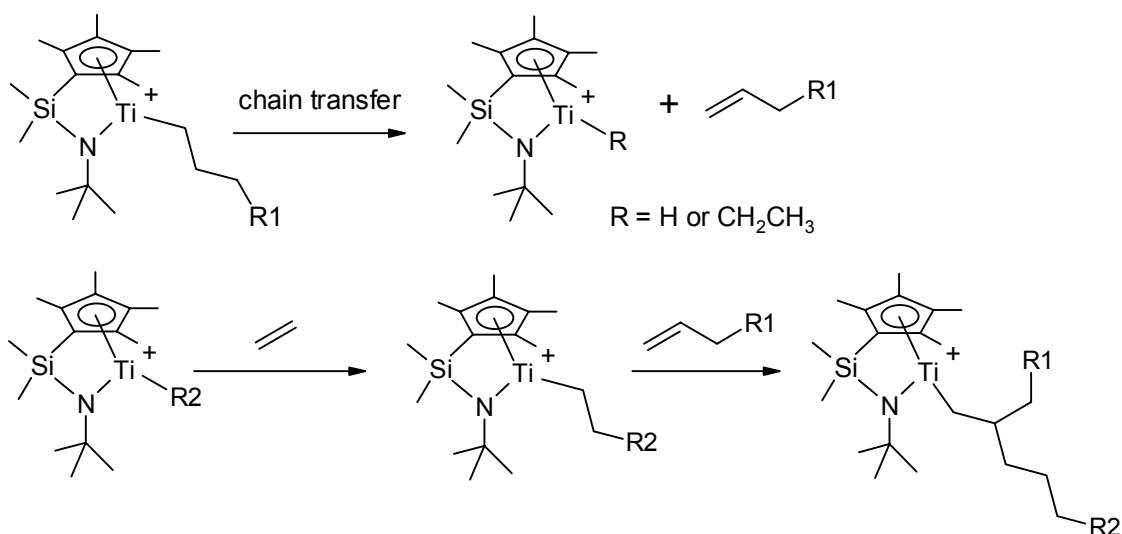
Ziegler-Natta catalyst based PE-HDs have a very linear structure. These polymers contain only a few short-chain branches and no LCB [8, p. 454]. Polyethenes produced with chromium catalysts have been found to contain small amounts of LCB according to ^{13}C NMR spectroscopical [9] and rheological measurements [10]. It has been reported [11] that the branched structure in the chromium based polyethenes results from the copolymerization reaction between ethene and macromonomer. This seems feasible: The chromium-catalyzed materials have a high vinyl content while the Ziegler-Natta -catalyzed polyethenes have mainly saturated end-groups [8 p. 454, 26].

Other means to induce LCB structure in the polyethene involve the post-reactor treatment, for example, by radiation [12, 13] or peroxide addition [14-16]. The branch structure may also originate from the thermoxidative decomposition [17, 18] if polyethene is exposed to unduly severe processing conditions.

2.2 Long-chain branching mechanisms

Terminal branching has been considered to be a very likely branching mechanism with metallocene catalysts [19-22]. The branching mechanism is shown in Scheme 2.1. According to this mechanism, the catalyst must first produce vinyl terminated polyethene chains, or macromonomers, and then copolymerize them into a growing polymer chain. Long-chain branching is believed to take place with this mechanism when a half-metallocene catalyst, Dow Chemical Company's constrained geometry catalyst (CGC), is used. The catalyst fulfills both prerequisites as it produces polyethene molecules with terminal double bonds and very efficiently copolymerizes ethene with 1-olefins [21, 23-25]. One manifestation of LCB formation via the macromonomer insertion route is the fact that the metallocene mediated copolymerization of ethene with nonconjugated dienes has been found to lead to cross-linking [26, 27].

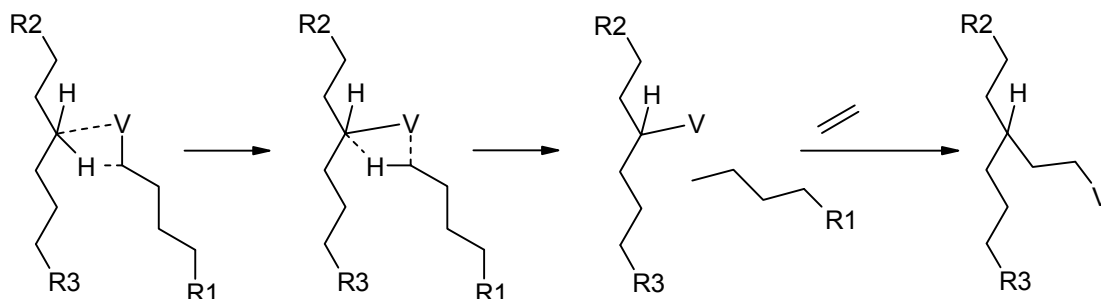
Scheme 2.1



However, it has been unclear whether the copolymerization route is generally effective in the formation of LCB structure with metallocene type catalysts. For this reason, it is necessary to understand both chain transfer mechanisms that determine end-group structures and the copolymerization abilities of metallocene catalysts.

The copolymerization reaction is not the only possibility for the production of the branched polymer. In the LCB polyethene obtained with a vanadium-based catalyst [11], the branching has been proposed to take place via alkane C-H activation. The proposed mechanism is shown in Scheme 2.2. The C-H bond activation mechanism is supported by the finding that *n*-hexane is reactive with the vanadium catalyst.

Scheme 2.2



2.3 Long-chain branching in single-center catalyzed polyethenes

Long-chain branching in metallocene-catalyzed polymers has been the subject of intense research since the first patents were published in the mid-nineties [19, 28]. The first single-site catalyst reported to produce LCB polyethene was the CGC, which is a half-metallocene [28, 29]. In the early publications, it was only stated that the open structure of CGC enables LCB formation. However, it has been possible to use sterically more hindered dicyclopentadienyl catalysts for the production of LCB polyethene. LCB has been produced with $\text{Cp}_2\text{ZrMe}_2/\text{B}(\text{C}_6\text{F}_4)_3$ [19] and $\text{Cp}_2\text{ZrCl}_2/\text{MAO}$ [V, 30, 33], nevertheless, the use of $(\text{Me}_5\text{Cp})_2\text{ZrMe}_2/\text{MAO}$ -catalyst resulted in a linear polymer [19]. In addition to these catalysts, $\text{Et}[\text{Ind}]_2\text{ZrCl}_2/\text{MAO}$ and other *ansa*-metallocenes have also been reported [31, 32, I, III-V] to produce LCB polyethene. Both supported [32] and homogeneous [I, 33] catalysts can be employed. Metallocenes produce LCB polyethene in gas-phase [31], slurry [I, 33], and solution systems [VIII].

Prior to the experimental work reported in paper [I], only patent literature was available on the LCB in single-site polyethenes. The first papers suggesting the presence of LCB in metallocene-catalyzed polyethenes were published in 1996 and 1998 [30, 32] followed by us [I]. The suggestions were based on ^{13}C NMR spectroscopy and rheological measurements. Figure 2.1 shows a ^{13}C NMR spectrum of a homopolyethene catalyzed with **1** and the peak assignment for LCB structure in the polymer [I]. The sample was estimated to contain ≈ 0.2 LCB / 1000 C.

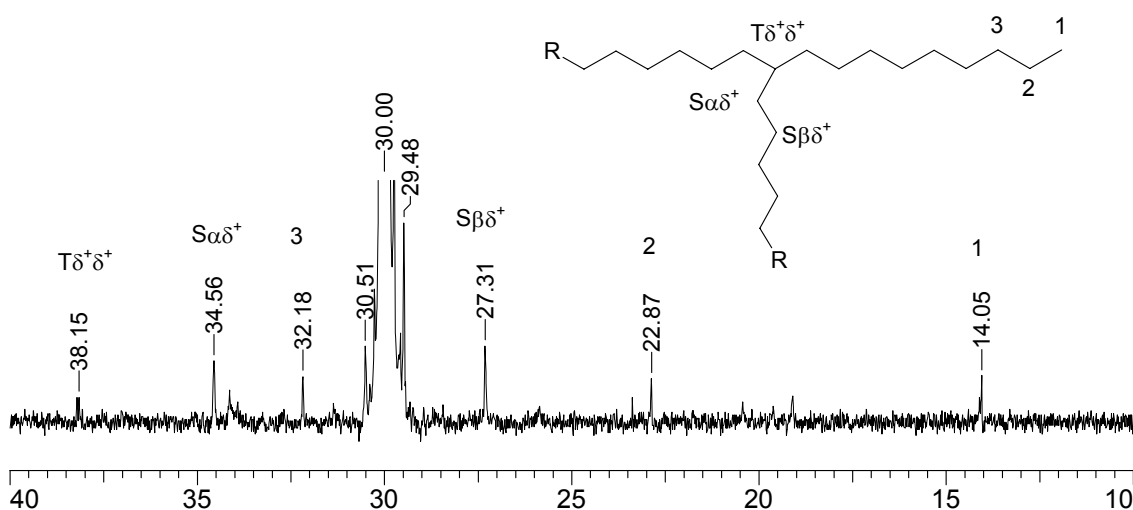


Figure 2.1 The ^{13}C NMR spectrum of a polyethene produced with $\text{Et}[\text{Ind}]_2\text{ZrCl}_2/\text{MAO}$ [I].

2.4 Rheological properties of long-chain branched polyethenes

Long-chain branching has several benefits relating to the polymer processability [34-37] since it affects the melt viscosity, temperature dependence of viscosity, melt elasticity, shear thinning, and extension thickening. The effect of the branching on the melt-state properties of polyethylene depends on the length and the distribution of the branches, and the molecular weight and the molecular weight distribution. In recent years, several research groups have intensively studied the rheological properties of LCB polyethylene [10, 30, 38-47].

The zero-shear viscosity (η_0) of polymers depends on the weight average molecular weight (M_w) as shown in Equation 2.1. The coefficient $\alpha \approx 3.4$ for a linear polymer when $M_w > M_c$ [34 p. 80, 35 p. 498]. Branched polymers have greater α values. Widely used k and α values for linear polyethylene at 190°C are $k = 3.4 \times 10^{-15}$ (Pa×s); $\alpha = 3.6$ [48]. At 150°C, the values $k = 6.8 \times 10^{-15}$ (Pa×s); $\alpha = 3.6$ have been reported [43].

$$\eta_0 = k \times M_w^\alpha \quad (2.1)$$

The effect of the branching on the melt viscosity is two-dimensional; 1) the decrease in the radius of gyration and 2) an increase in the entanglement density. Depending on the dominant component, the LCB decreases or increases the η_0 [49]. The branch length and distribution depends on the branching mechanism, which thus has a large effect on the observed η_0 [7, 50].

The melt rheological properties of selected LCB metallocene-catalyzed samples are shown in Table 2.1 [I]. The reference samples are used for comparison purposes. Ref-1 is a (*n*-BuCp)₂ZrCl₂-catalyzed PE-HD, whose structure is considered to be very linear. Ref-2 is a commercial Ziegler-Natta based PE-LLD that contains only SCB and ref-3 is a conventional PE-LD sample that contains a considerable amount of LCB.

The complex viscosity (η^*) of a linear polymer, at low shear rate (or at low frequency), approaches η_0 , which depends on the M_w . The comparison of the GPC based M_w and $\eta^*(0.02 \text{ rad/s})$ of B2 and ref-1 reveals a clear discrepancy. The η^* of B2 is 2-fold compared to that of ref-1, though, the M_w of B2 is less than 50% of the M_w of ref-1. The same discrepancy is seen between B3 and ref-2. The discrepancy is readily explained by branching, which increases the η_0 dramatically [I].

Table 2.1 Melt rheological properties of linear and branched polyethenes [I].

Sample	Polymer Type	M_w [kg/mol]	M_w/M_n	$\eta^*(0.02 \text{ rad/s})$	E_a [kJ/mol]
				at 190°C [Pa×s]	
B2 ^a	PE-LLD	153	3.6	710,000	64
B3 ^a	PE-LLD	78	3.3	13,000	59
D1 ^b	PE-HD	114	2.2	26,000	41
D3 ^b	PE-LLD	140	2.3	29,000	39
Ref-1	PE-HD	380	2.1	307,000	26
Ref-2	PE-LLD	100	3.8	5,500	33
Ref-3	PE-LD	154	9.3	4,600	55

^a Polymerized using $\text{Et}[\text{Ind}]_2\text{ZrCl}_2/\text{MAO}$ as a catalyst.

^b Polymerized using $\text{Et}[\text{H}_4\text{Ind}]_2\text{ZrCl}_2/\text{MAO}$ as a catalyst.

Viscosity measurement alone does not prove the presence of LCB. The temperature dependence of viscosity, or the Arrhenius type of flow activation energy (E_a), is considered to be a very reliable and sensitive measure of LCB in polyethene [49, 51, 52]. The increased length and content of the branches increases the E_a , which is not affected by the breadth of M_w/M_n . The E_a of linear polyethene is 25-29 kJ/mol [14, 53], a small amount of SCB results in E_a values of 30-35 kJ/mol [38, 52, 54] and LCB polyethene has E_a values of 40-60 kJ/mol [14, 52].

The values shown in Table 2.1 are in line with the reported values. Linear PE-HD, ref-1, has an E_a value of 26 kJ/mol. PE-LD (ref-3), which is known to contain LCB has an E_a value of 55 kJ/mol. The experimental materials (B2, B3, D1, D3) have clearly elevated E_a values, ranging from 40 to 60 kJ/mol, strongly supporting the presence of LCB in these materials [I].

A peculiar effect of the LCB is the shear rate dependence of E_a [55]. The E_a of LCB polymer decreases with increasing shear rate. E_a of linear polymers is independent of the shear rate. This behavior is attributed to the relaxation [52] and disentanglement [55] process of the branched chains. At the higher shear rate entanglements of the branched polymers are more easily detached than the entanglements of the linear chains.

Besides the effect on the η_0 and E_a , the LCB influences the viscosity curve together with the M_w/M_n , enhancing the shear thinning and melt elasticity [15, 56, 57]. The high M_w fraction of the polymer has the largest influence on this [34 p. 372].

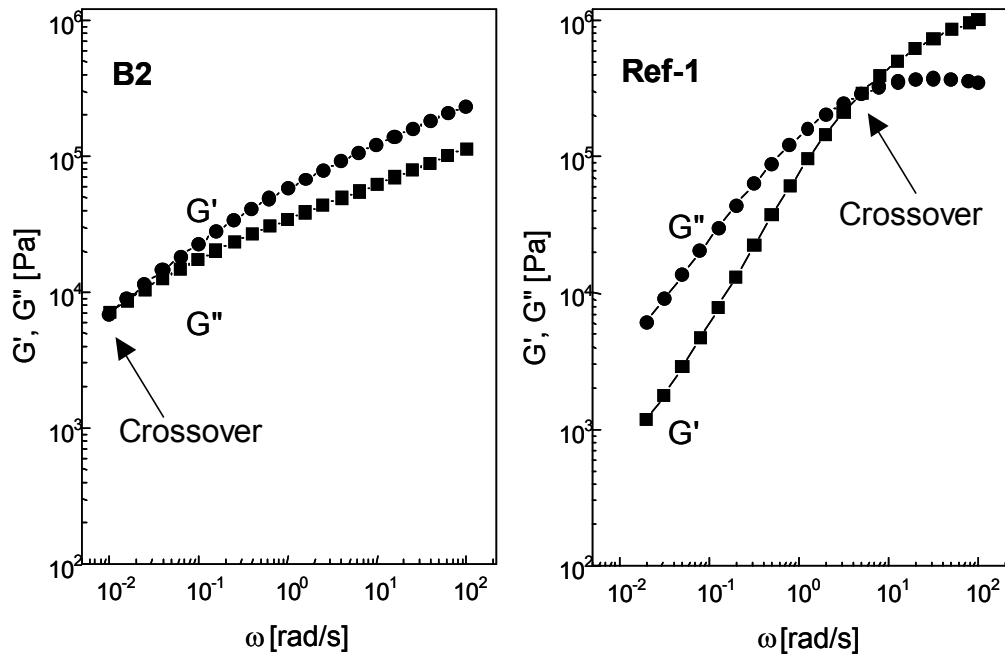


Figure 2.2. Melt elasticity (G' vs. G'') curves of a long-chain branched (B2) and linear (ref-1) polyethylene. Long-chain branching increases the value of storage modulus (G') and shifts the crossover to lower frequency and moduli values [I].

Figure 2.2 shows the effect of LCB on the melt elasticity, or the relative contributions of storage (G') and loss (G'') moduli. [I] For a linear polymer with narrow M_w/M_n , G' is much less than G'' at low frequencies. An increase in the LCB or M_w/M_n shifts the crossover to lower frequencies and modulus values. For sample B2, the G' is already equal to the G'' at the low angular frequency range due to LCB.

In extensional flow, when the polymer melt is drawn, the LCB has one more interesting effect on the stress-strain curve. The LCB induces strain hardening, or extension thickening, with increasing strain rate. The resulting elongational viscosity (η_E) can reach a maximum value, which is 3-7 times higher than the η_E at a low strain rate. After the maximum value, extension thinning takes place [34 pp. 231-268]. The η_E of the linear polymer shows only extension thinning behavior.

3 POLYMERIZATION MECHANISMS

Understanding the mechanisms and kinetics involved in the polymerization process enables one to predict the structure of the polymer formed. Propagation and termination rates determine molecular weight, molecular weight distribution, and, in copolymerization, comonomer content and distribution. The catalyst initiation and deactivation processes have an influence on the kinetics, and the cocatalyst may have an effect on the extent of the prevailing mechanisms [3, 5, 6, 58, 59].

3.1 Initiation and propagation reactions

A simplified scheme for the catalyst activation and propagation mechanism in metallocene-catalyzed polymerizations is shown in Table 3.1. Neutral metallocene compound (L_2MCl_2) is inactive without an activator and requires a strong Lewis acid (i.e. methylaluminoxane) to form a cationic metal center, which is active in 1-olefin polymerization [58, 59]. Propagation then proceeds by 1-olefin coordination and insertion via a transition state [5, 60, 61]. The exact route for the monomer insertion is not completely understood. Agostic interactions [62] appear to have an important role in the chain growth process.

Kinetic studies [5, 63, 64] have shown that the polymerization rate R_p , does not always follow a simple first order relationship ($\alpha = 1$), but often depends on the monomer concentration to the power 1.2-1.4, indicating complex reaction pathways. Different kinetic models have been proposed to describe this kind of polymerization behavior [5, 65, 66].

Table 3.1 Schematic activation and propagation reactions and the kinetic equation for propagation. Propagation constant includes the active site concentration ($k_p = k_p'[C^*]$). L = ligand; MAO = methylaluminoxane; M = Ti, Zr, or Hf

Reaction	Reaction path	Kinetic Expression
Activation	$L_2MCl_2 + MAO \rightarrow L_2M^+-CH_3 + [MAO-Cl_2]^-$	
Propagation	$L_2M^+-CH_2CH_2R + CH_2=CH_2 \rightarrow L_2M^+-CH_2CH_2CH_2CH_2R$	$R_p = k_p \times [M]^\alpha$

3.2 Chain transfer reactions

The most common chain transfer mechanisms identified in metallocene catalyzed ethene polymerization and the corresponding end group types have been collected in Table 3.2.

β -H elimination (chain transfer to the metal) and chain transfer to the monomer are generally believed to be the dominant chain transfer reactions in the olefin homopolymerization [5, 67, 68]. They lead to the formation of vinyl ($\text{CH}_2=\text{CH}-\text{R}$) or vinylidene ($\text{CH}_2=\text{C}(\text{R}')-\text{R}$) bond in ethene or 1-olefin polymerization, respectively. There is some theoretical [23] and experimental [69] evidence that chain transfer may take place via alkene C-H activation (σ -bond metathesis) for some polymerization systems. In that case, vinyl bond is at the beginning of a chain.

In propene polymerization, β - CH_3 elimination can take place with some catalyst systems, which leads to the formation of allyl ($\text{CH}_2=\text{CH}-\text{CH}_2-\text{CH}(\text{CH}_3)-\text{R}$) end-groups [70].

Table 3.2 Chain transfer reactions, schematic reaction path, and the kinetic equations in ethene polymerization. Chain transfer constant include the active site concentrations ($k_{\text{tr}} = k_{\text{tr}}'[\text{C}^*]$). Ligands have been omitted for clarity.

Chain transfer reaction	Reaction components	End-groups	Kinetic expression
Chain transfer to monomer	$\text{M}^+-\text{CH}_2\text{CH}_2\text{R} + \text{CH}_2=\text{CH}_2$	$\rightarrow \text{M}^+-\text{CH}_2\text{CH}_3 + \text{CH}_2=\text{CHR}$	$R_{\text{tr,M}} = k_{\text{tr,M}}[\text{M}]$
β -H elimination	$\text{M}^+-\text{CH}_2\text{CH}_2\text{R}$	$\rightarrow \text{M}^+-\text{H} + \text{CH}_2=\text{CHR}$	$R_{\text{tr},\beta\text{-H}} = k_{\text{tr},\beta\text{-H}}$
Chain transfer to aluminum	$\text{M}^+-\text{CH}_2\text{CH}_2\text{R} + \text{AlR}'_3$	$\rightarrow \text{M}^+-\text{R}' + \text{R}'_2\text{AlCH}_2\text{CH}_2\text{R}$	$R_{\text{tr,Al}} = k_{\text{tr,Al}}[\text{Al}]$
Chain transfer to hydrogen	$\text{M}^+-\text{CH}_2\text{CH}_2\text{R} + \text{H}_2$	$\rightarrow \text{M}^+-\text{H} + \text{CH}_3\text{CH}_2\text{R}$	$R_{\text{tr,H}_2} = k_{\text{tr,H}_2}[\text{H}_2]$
σ -bond metathesis	$\text{M}^+-\text{CH}_2\text{CH}_2\text{R} + \text{CH}_2=\text{CH}_2$	$\rightarrow \text{M}^+-\text{CH}=\text{CH}_2 + \text{CH}_3\text{CH}_2\text{R}$	$R_{\text{tr},\sigma} = k_{\text{tr},\sigma}[\text{M}]$

Chain transfer to the aluminum (cocatalyst) is usually of minor importance in ethene polymerization. However, it appears to be more important in propene polymerization [71]. Chain transfer to the aluminum leads to the formation of an Al-CH₂-R compound. The aluminum-alkyl bond is highly reactive and the treatment with HCl/EtOH – a standard laboratory washing procedure – results in a saturated end-group in the polymer [72].

Chain transfer to an external chain transfer agent, for example hydrogen [67, 73], results in a saturated chain end. The introduction of hydrogen significantly increases the productivity of some metallocene catalysts, especially in propene polymerization [74, 75]. Hydrogen is far more reactive in metallocene-catalyzed polymerizations than in Ziegler-Natta polymerizations [76].

In the copolymerization of ethene and 1-olefin, vinylidenes and *trans*-vinylenes (CH₃-R'-CH=CH-R) account for a significant part of the end-groups. Both β-H elimination and chain transfer to the 1-olefin after 1,2-insertion of the 1-olefin results in the formation of a vinylidene bond. β-H elimination or chain transfer to the monomer after 2,1-insertion results in the formation of a *trans*-vinylene bond in the polymer chain [77].

3.3 Isomerization reactions

Isomerization reactions play an important part in the formation of regio- and stereoerrors in propene polymerization and in chain termination [75, 78-80]. The isomerization reactions contribute not only to the formation of stereo errors but also to the chain transfer. The catalyst structure [81] and monomer concentration [82] have a major influence on the extent of the isomerization reaction leading to the formation of the stereo errors.

In ethene polymerization, isomerization reactions have a less important role. There are some reports of the formation of short chain branching and *trans*-vinylenes via isomerization reactions. Small quantities, up to 1.4 mol-%, of ethyl branches [83] have been found in *meso*-Et[Ind]₂ZrCl₂/MAO catalyzed polyethenes. Small amounts of quaternary ethyl branches have also been found [84]. Branching was proposed to take place via β-H transfer to the coordinated ethene and reinsertion. Ethyl branching has also been reported to occur with other catalyst systems [IV, VII, VIII, 85].

Short-chain branching in the polyethenes produced with Brookhart type Ni- and Pd-catalysts originates from a chain-walking mechanism [86, 87]. ^{13}C NMR spectroscopic experiments have shown that methyl branches dominate and the fraction of longer branches is inversely proportional to the length of a branch [88]. There are no reports as to whether these polymers contain branches long enough to be considered rheologically significant.

The presence of methyl branches [24, **VII**, **VIII**] and *trans*-vinylenes [89-91, **III**] in polyethenes could be explained with an isomerization reaction that includes a chain transfer reaction (β -H elimination or chain transfer to monomer) and olefin rotation. Subsequent 2,1-reinsertion of polymer chain would result in the formation of a methyl branch. Alternatively, chain transfer can take place, which would lead to the formation of a *trans*-2-vinylene end group. The latter reaction would have a significant influence on the vinyl end-group selectivity [79, 89-92].

A source for internal unsaturations (*trans*-vinylenes) could be a hydrogen evolution mechanism [93] or 2,1-insertion of macromonomer and subsequent termination [94]. According to the proposed hydrogen evolution mechanism, 2,1-insertion of the comonomer is followed by β -H elimination. Then, dehydrogenation takes place via an allylic intermediate. Further chain growth results in the internal *trans*-vinylene in a polymer chain and free hydrogen in the polymerization reactor. This mechanism has been proposed to explain the internal *trans*-vinylenes in ethene–1-olefin copolymers obtained with $\text{Ph}_2\text{Me}[\text{Cp}][\text{Flu}]\text{ZrCl}_2/\text{MAO}$. Hydrogen can react further, eventually leading to the formation of saturated chain ends.

The internal *trans*-vinylene bond formation via 2,1-insertion of macromonomer appears to be more improbable. One might expect to observe more 1,2-insertion induced (long-chain) branches than 2,1-insertion induced *trans*-vinylenes in a polymer chain. However, *trans*-vinylene content is often higher than the branch content.

4 POLYMERIZATION PARAMETERS INFLUENCING THE MICROSTRUCTURE OF POLYOLEFINS

The analysis of the polymer microstructure and end-groups reveals the fingerprints of the mechanisms involved in the polymerization process. The presence of the different end-group types indicates that various chain transfer or isomerization reactions have participated in the polymerization. However, different mechanisms may produce the same end group types. In these cases, the response to the changes in polymerization conditions may be utilized to reveal the reaction paths. The response to the polymerization temperature, monomer, comonomer, cocatalyst, and hydrogen concentration depends largely on the catalyst system.

The microstructure of polypropene has been thoroughly studied but little information is available regarding the influence of the polymerization conditions on the structure of polyethylene. The main reason for this is the richness of microstructural details in polypropene. In addition to this, due to the large number of catalyst structures developed during the last decade, much effort has been put into catalyst comparison and the effect of polymerization conditions has gained less attention. Based on polypropene data, some general trends regarding the influence of the polymerization conditions on the polymer microstructure can be observed.

4.1 Temperature

In ethene polymerization, the *trans*-vinylene content has been found to increase with polymerization temperature [90]. In propene polymerization, the isotacticity of polypropene decreases with an increase in the temperature [95]. The decrease in the stereospecificity at elevated temperatures is caused by an increased number of isomerization reactions after stereoregular 1,2-insertion [78]. The total amount of regioirregular insertions does not seem to change, though 2,1-inserted monomers isomerize in larger quantities to the 1,3-position at high temperatures [78]. In a similar way, the fraction of stereoirregular vs. stereoregular insertions increases relatively slowly with temperature [95]. A small temperature dependence can be expected at a large temperature interval because the rigidity of a catalyst ligand changes slightly.

4.2 Monomer concentration

Monomer concentration may have an effect on the molecular weight, depending on the chain transfer mechanism. If a unimolecular chain transfer reaction dominates, i.e. β -H elimination, the chain transfer rate is independent of the monomer concentration and an increase in the concentration increases the molecular weight. If a bimolecular chain transfer reaction dominates, i.e. chain transfer to the monomer, the chain transfer rate increases proportionally with the propagation rate and the molecular weight is independent of the monomer concentration.

In ethene polymerization, lowering the ethene concentration has been found to keep the ethyl branch content constant [83], increase *trans*-vinylene bond content [89, 91], and increase the methyl branch content [VII].

Decreasing the propene concentration in the polymerization medium lowers the isotacticity of polypropene when C_2 -symmetric [81] metallocene catalysts are used. This is due to the isomerization reactions. With some C_1 -symmetric catalysts the trend has been found to be opposite: An increase in the monomer concentration decreases isotacticity [96, 97]. This has been proposed to be caused by the increase in stereoirregular insertions [97]. The C_1 -symmetry enables propene to be inserted stereoregularly from one-side only. At low monomer concentration, a back-skip reaction [98], in which a growing chain flips to the sterically less restricted coordination-site, has enough time to occur. As the monomer concentration is increased, the monomer has a greater possibility to intercept this flipping and insert in a stereoirregular fashion [97].

4.2.1 The effect of ethene concentration on the vinyl selectivity and molecular weight

Vinyl selectivity is considered to be an important factor in LCB formation. Figure 4.1 shows the vinyl bond contents of polyethenes produced with catalysts **1-8**. In addition to the vinyl end-groups, the polymers contained *trans*-vinylenes and a very small amount of vinylidene double bonds [II, III, V].

The reaction paths for *trans*-vinylene formation were discussed in Chapter 3.3. Vinylidene bonds may originate from a side-reaction: a vinyl terminated polyethene macromonomer is reincorporated into a growing chain, followed by a subsequent termination [III, 94].

Vinyl selectivity was almost 100% with the indenyl substituted Zr-catalysts **1**, **7**, **8**, and **5**. A decrease in the monomer concentration slightly lowered the vinyl selectivity. Intermediate vinyl selectivities were observed with **3** and **4**. The polyethenes produced with the latter catalyst typically had much higher vinyl contents than those produced with **3**. The lowest vinyl selectivities and vinyl contents were in **2** and **6** based polyethenes, where only a third of the molecules contained vinyl bonds.

Figure 4.2 shows the M_n as a function of ethene concentration (C_E). **1**, **5**, **7**, and **8** produced polyethene with a constant M_n . The M_n of polyethenes catalyzed by **2**, in turn, increased proportionally with the C_E . The M_n dependence of polyethenes produced with **3**, **4**, and **6** appears to lie somewhere between these two cases. The data from vinyl end-group and molecular weight analysis was utilized in the determination of chain transfer mechanisms, which is discussed in Chapter 4.4.

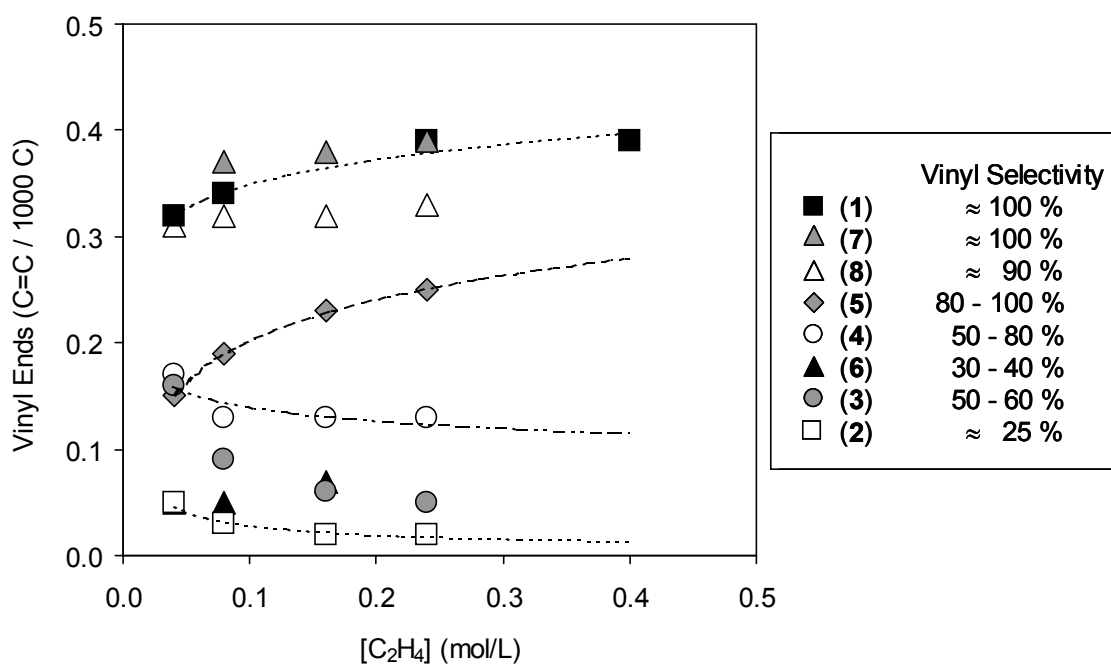


Figure 4.1 The vinyl end group content and selectivity in homopolyethenes produced with catalysts **1-8**. Vinyl selectivity has been calculated from the GPC (M_n) and FTIR data. Polymerization conditions: $T = 80^\circ\text{C}$, MAO cocatalyst, solvent toluene. Trendlines are for guidance only.

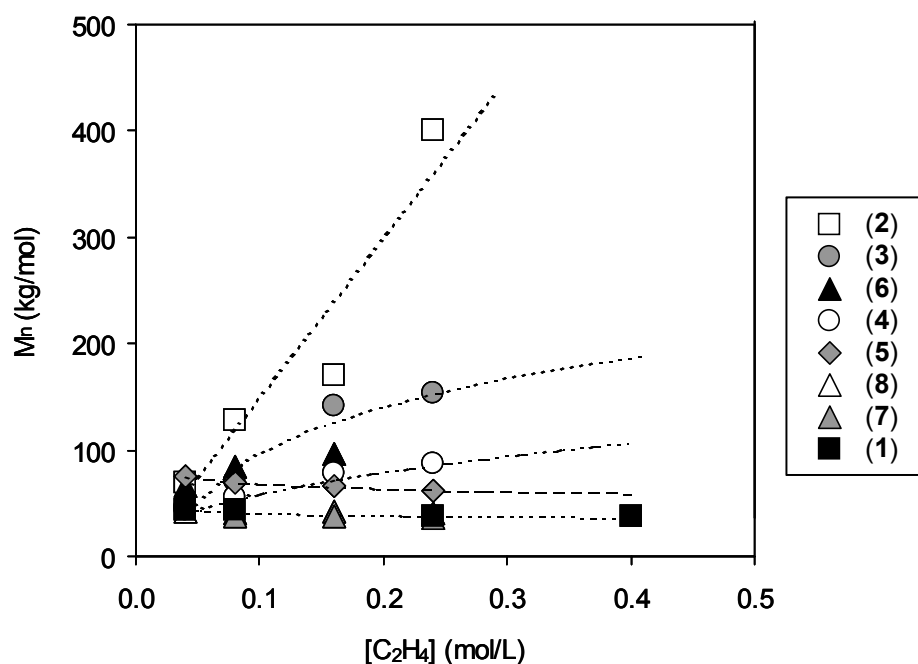


Figure 4.2 The number average molecular weight of homopolyethenes as a function of ethene concentration. Polymerization conditions: $T = 80^{\circ}\text{C}$, MAO cocatalyst, solvent toluene. Trendlines are for guidance only.

4.2.1 The effect of ethene concentration on the molecular weight distribution

In the ethene polymerization with **1**, a decrease in the C_E resulted in a small increase in the M_n and a very pronounced increase in the M_w/M_n [III]. Figure 4.3a illustrates this. Similar behavior was observed with the other bis(indenyl) catalysts **5**, **7**, and **8**. At $C_E = 0.40$ M polymerized polyethene had a M_w/M_n of about 2.0. With decreasing C_E , a shoulder appeared to the high M_w tail, and for a polymer produced at the lowest C_E the M_w/M_n was 3.2. The broadening may have arisen from the presence of multiple active sites, or other factors.

The GPC chromatogram curve of the sample produced at $C_E = 0.02$ M was found to fit in the Schulz-Flory distribution model, with three different active centers. Generally, metallocene catalysts have been considered to exhibit only one kind of active center. The introduction of hydrogen or comonomer (1-olefin) should result in a broader M_w/M_n , or reveal multiple peaks in the DSC curves if three different active species were present. The experiments with 1-olefin or hydrogen, however, gave narrow GPC and unimodal DSC melting curves. Therefore, the presence of three active centers is considered unlikely.

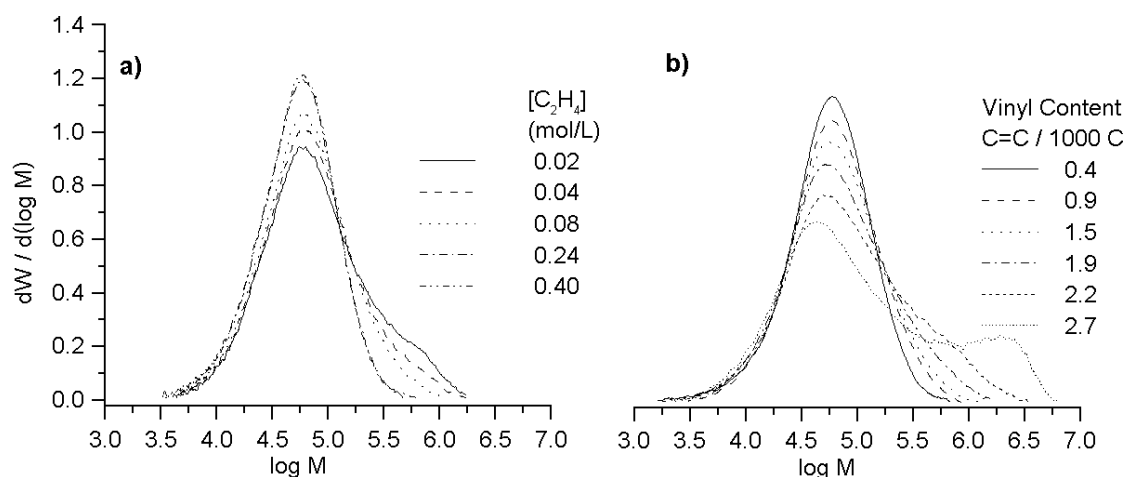


Figure 4.3. a) The ethene concentration effect on the molecular weight distribution of 1/MAO catalyzed polyethenes. $T_p = 80^\circ\text{C}$. [III] b) The diene concentration effect on the molecular weight distribution curve ($C_E = 0.24 \text{ mol/L}$) [VI]. Macromonomer reincorporation is believed to lead the formation of the high M_w tail.

A more likely explanation for the broadening of the M_w/M_n at the high M_w tail is the reincorporation of a vinyl-terminated macromonomer into a growing polymer chain. This reaction would lead to the formation of very long linear chains or branched polymer [III]. Measurement with a dual-detector GPC indicated the presence of branching in the high M_w tail.

This conclusion is further supported by the results obtained in ethene copolymerization with a nonconjugated α,ω -diene [VI]. The use of an α,ω -diene produces polyethene chains with vinyl bonds along the polymer backbone. Figure 4.3b shows the effect of increasing diene content on the M_w/M_n . Homopolyethene (0.4 C=C / 1000 C) had a narrow M_w/M_n but an increase in the vinyl bond content resulted in the formation of a high molecular weight tail. This indicated that very long chains had been incorporated into a growing polymer chain. In addition, the melt rheological measurements revealed that the branching increased with decreasing C_E or increasing diene content (see chapter 6).

4.3 The effect of hydrogen

Hydrogen acts as a chain transfer agent in olefin polymerization, reducing the molecular weight, but the response varies from one catalyst to another [75, 99]. Incorporation of hydrogen does not affect the isotacticity of polypropene [75], but it drastically

diminishes the amounts of regio errors [68], since a slow propagation rate after 2,1-insertion of the monomer facilitates hydrogen insertion and chain transfer [75, 78]. In ethene polymerization, hydrogen has been found to efficiently suppress the formation of *trans*-vinylenes, while the effect on the vinyl bonds is less pronounced [99, **III**, **V**].

The catalysts had marked differences in sensitivity towards hydrogen insertion and the resulting chain transfer. The hydrogen sensitivity of catalysts **1-6** is collected in Table 4.1 [**III**, **V**]. When **2** or **3** was used, the molecular weight decreased drastically and the vinyl bond content (C=C / chain) was very low. The decrease in the molecular weight was also very notable with **4** and **6**. Bis(indenyl) substituted catalysts **1** and **5** had the lowest tendency towards hydrogen insertion under these polymerization conditions [**III**, **V**].

Table 4.1. The effect of hydrogen on the polyethene structure.^a

Catalyst	Hydrogen Feed (mmol)	M _w (kg/mol)	M _n (kg/mol)	M _w /M _n	<i>trans</i> -Vinylenes (C=C / 1000 C)	Vinylns (C=C / 1000 C)
1	0.0	98	41	2.4	0.03	0.37
1	1.3	46	25	1.9	0.00	0.36
2	0.0	300	128	2.3	0.08	0.03
2	^b 0.0	1000	400	2.5	<0.06	<0.02
2	^b 0.4	69	34	1.9	0.00	0.02
3	0.0	290	130	2.3	0.05	0.07
3	0.5	17	8	2.1	0.00	0.08
4	0.0	142	46	2.4	0.05	0.13
4	1.3	18	9	2.0	0.00	0.20
5	0.0	167	65	2.6	0.02	0.19
5	1.3	91	37	2.4	0.00	0.17
6	0.0	292	85	3.4	0.03	0.05
6	1.3	45	21	2.2	0.00	0.03

^a Polymerization conditions: T = 80°C; C_E = 0.08 mol/L; cocatalyst MAO.

^b C_E = 0.24 mol/L.

The difference in the sensitivity towards chain transfer was attributed to the dominance of competing chain transfer mechanisms [III]. After hydrogen insertion, the active site is of form Zr^+-H . Similarly, β -H elimination inherently produces Zr^+-H bonds but chain transfer to the monomer produces $Zr^+-CH_2CH_3$ bonds. Apparently, for **2** the energy barrier for the formation of Zr^+-H bond is lower than required for the formation of $Zr^+-CH_2CH_3$ bond. The situation is opposite for **1** and **5**. Analogously considering the hydrogen insertion, the formation of Zr^+-H bonds is more difficult for **1** or **5** than for **2**, which would explain the difference in sensitivity towards chain transfer to hydrogen.

4.4 Chain transfer mechanisms in examined catalysts

Based on the polymerization studies, several conclusions regarding the polymerization behavior and prevailing chain transfer mechanisms can be drawn. The conclusions are summarized in Table 4.2, which highlights the differences between the catalysts under similar reaction conditions.

Table 4.2 Comparison of the relative magnitudes of chain transfer mechanisms, isomerization tendency, and hydrogen reactivity of the examined catalysts in ethene polymerization at 80°C. Isomerization tendency describes the observed *trans*-vinylene content.

Catalyst	Chain transfer to the monomer	β -H Elimination	Chain transfer to the aluminum	Isomerization tendency	Reactivity towards H ₂	
1	+++	-	-	+	+	
2	-	++	+	+++	+++	
3	o	+	+	++	+++	
4	+	o	+	++	++	
5	+++	-	o	+	+	
6	o	+	+	++	++	
7	+++	-	-	o	n.d.	
8	+++	-	-	+	n.d.	
+++	very important		++	important	+	moderately important
o	may have some importance		-	not important	n.d.	not determined

In ethene homopolymerization, chain transfer to monomer, β -H elimination, and chain transfer to cocatalyst are catalyst specific [II-V]. One should also note that reactant concentrations have a significant effect on the relative importance of the corresponding chain transfer reaction.

The chain transfer to the monomer was judged to be the major chain transfer mechanism with the *ansa*-bis(indenyl) zirconium catalysts **1**, **5**, **7**, and **8**. This conclusion was based on the following two findings: 1) Vinyl selectivity was approximately one unsaturation in each chain, (Fig. 4.1) which suggested that chain transfer to MAO was negligible, and 2) the M_n was independent of ethene concentration, (Fig. 4.2) which meant that β -H elimination was insignificant.

β -H elimination was a dominant chain transfer mechanism with **2**. (Fig. 4.2) The M_n increased proportionally with the ethene concentration, and the vinyl end-group selectivity was constant. Low vinyl end-group selectivity suggested that isomerizations decreased the vinyl end-group selectivity, or chain transfer to aluminum was present to some degree.

Possibly, all three chain transfer routes were equally competing with **3**, **4**, and **6**. The M_n of polyethenes produced with these catalysts depended, more or less, on the ethene concentration, and the vinyl end-group selectivity was clearly less than 100%.

Isomerization tendency appeared to be the most significant with the catalysts in which β -H elimination dominated and the hydrogen reactivity was high.

The tendency towards chain transfer to hydrogen was the highest with **2** and **3**. Catalysts **4** and **6**, and the *ansa*-bis(indenyl) catalysts, **1** and **5**, had the lowest response.

5 COPOLYMERIZATION OF ETHENE AND 1-OLEFINS

In this work, copolymerization studies were used to predict the relative reactivity of very long 1-olefins with various metallocene compounds [II-VI]. Ethene-co-1-hexene and ethene-co-1-hexadecene copolymers were produced using known (1-6) and novel siloxy-substituted (7-10) metallocene catalysts. The reactivity ratios of the components are listed in Tables 5.1 and 5.2.

Metallocene catalysts have successfully been applied for the copolymerization of ethene and various short and long 1-olefins, for example 1-octadecene [100] and vinyl-terminated polypropene oligomers ($M_n \approx 700$ g/mol) [101]- Bulky comonomers, i.e. norbornene and styrene [6], and isobutene [102] are also reactive to some extent.

Ethene is the most reactive olefin. The reactivity of 1-olefins decreases as the length of the alkyl group is increased. However, the difference in the reactivity diminishes as the length is increased. The linear 1-olefins are more reactive than the branched 1-olefins; the branching at the α -carbon decreases the reactivity drastically. The poor reactivity of the α -substituted 1-olefins is generally attributed to the steric crowding in the vicinity of the reactive double bond. The reactivity of other branched and bulky 1-olefins depends largely on their structure [103 p. 140].

Apart from these general reactivities of various 1-olefins, the reactivity of a 1-olefin is highly dependent on the catalyst structure. Krentsel *et al.* [103 p. 248] have summarized the literature published on the reactivity ratios for several Ti, Cr, and V based traditional transition-metal catalysts and novel metallocenes. Metallocene catalysts are generally more reactive towards comonomer insertion than traditional transition metal catalysts for olefin polymerization, but the reactivity of a 1-olefin is highly dependent on the ligand structure of metallocene complex.

Table 5.1 Reactivity ratios for ethene/1-hexene and ethene/1-hexadecene at 80°C [II, III, V, VI].

Catalyst	1	2	3	4	5	6	7	8	
{	r_{ethene}	48±4	71±4		112±9	26±4	6±1	55±3	19±4
	$r_{1\text{-hexene}}$	<0.02	<0.03					0.005	0.006
{	r_{ethene}	51±7		160±13				63±2	25±1
	$r_{1\text{-hexadecene}}$							0.002	

Table 5.2 Reactivity ratios for ethene and 1-hexene [IV] at 40°C.

Catalyst	7	8	9	10	
{	r_{ethene}	36±3	16±1	11±1	10±1
	$r_{\text{1-hexene}}$	0.003	0.005	0.005	0.001

5.1 Influence of the ligand structure on comonomer reactivity

The copolymerization series carried out in this study (Table 5.1) is an attempt to summarize the copolymerization behavior of some common metallocene catalysts. Overall, the results agree with the general trends reported in the literature. Direct comparison of the literature data regarding the copolymerization abilities of metallocene catalysts is difficult, as the copolymerization studies with longer 1-olefins have usually been carried out with a limited selection of catalysts under different polymerization conditions [85, 93, 101, 104-107]. Furthermore, some comparisons provide contradictory data. The discrepancies may arise from poor control of the polymerization conditions. Therefore, the literature values should be treated with caution if no adequate background information for the polymerization method has been provided.

Electronic factors at the active center and steric environment in the vicinity of the active center of a metallocene catalyst determine the reactivity of monomers and the structure of the copolymer. Many general conclusions about the influence of the ligand structure on the polymer structure [108, 109] can be made, although the details of how the combination of electronic and steric effects determines the reactivities of reactants are unknown. Ligand substitution, transition metal (Ti, Zr, Hf), and the interannular bridge have distinctive effects on the polymerization behavior. Hafnium-based catalysts are considered to exhibit better copolymerization properties than zirconium based catalysts [110].

The basic zirconocene, Cp_2ZrCl_2 (**4**), is highly reactive towards ethene and moderately reactive towards 1-olefin (comonomer) insertion [111]. The structure of the catalyst does not hinder free rotation of the cyclopentadienyl ligands. Furthermore, the substituent-free cyclopentadienyl ligands do not promote any stereocontrol for the 1-olefin coordination. Free rotation leads to a dramatic decrease in the 1-olefin response

with increasing polymerization temperature and the lack of stereocontrol results in misinsertions, which inhibit the chain growth and decrease the molecular weight drastically. Polypropene produced with this catalyst is atactic and has a low molecular weight [108].

The introduction of an interannular bridge between the ligands eliminates the free rotation and the substitution of the cyclopentadienyl with a C_2 -symmetric ligand promotes stereocontrol for 1-olefin insertion. *rac*-Et[H₄Ind]₂ZrCl₂ (**2**) and *rac*-Et[H₄Ind]₂TiCl₂ were the first metallocene catalyst shown to produce isotactic polypropene [112, 113]. This catalyst has also clearly higher comonomer response than **4** [104, 114.]

The rigid structure of **2** prevents the regio- and stereoirregular insertions to a large extent. This is very true at low temperatures. At higher temperatures the stereocontrol effect is weakened [95]. The dehydrogenation of the tetrahydroindenyl ligand provides a less restricting indenyl ligand; the indenyl ligand forms a plane. *rac*-Et[Ind]₂ZrCl₂ (**1**) produces more isotactic polypropene at low monomer concentration [75] and at a higher temperature than **2** [95]. Also, **1** exhibits better copolymerization ability than **2** [115, **III**]. The electronic effects may also play a role in the better 1-olefin response. The electronic density around the central metal is lowered [116] when the alkyl ligand is replaced with an aromatic ligand.

Other means of improving the comonomer reactivity is a variation of the length of the interannular bridge. In propene polymerization, replacing the –CH₂CH₂– bridge with a shorter –Si(Me₂)– bridge increases the molecular weight and isotacticity. [117] *rac*-Me₂Si[Ind]₂ZrCl₂ (**5**) has also higher comonomer response than **1** [V] or **2** [104].

Recent advances in catalyst design have resulted in more sophisticated catalyst structures with improved copolymerization abilities. The metallocene *rac*-Me₂Si[Me-Benz[e]Ind]₂ZrCl₂ is one example [118, 119]. This catalyst was originally developed for isotactic polypropene production, but it displays also a better copolymerization ability than **5** [120].

Other examples are provided by the introduction of heteroatoms (N, O, S, P) as ligand substituents, which has resulted in novel metallocene complex families. Increased comonomer response could be achieved with a proper siloxy-substitution on an indenyl ligand. [**II**] For example, the use of *rac*-Et[3-*tert*-BuSiMe₂OInd]₂ZrCl₂ (**8**) results in an almost 3-fold increase in the comonomer incorporation compared to the corresponding 2-siloxy-substituted catalyst **7** or **1**. The importance of heteroatom

substitution is highlighted by comparing the copolymerization behavior of two catalysts with different ligands, [3-*tert*-BuSiMe₂Oind] vs. [3-*tert*-BuSiMe₂Ind]. The results have shown that the latter silyl substituted catalyst has a poor comonomer response, probably due to the steric crowding [121].

Still another interesting improvement in the comonomer response has been achieved using *meso*-isomers of C₂-symmetric metallocenes. [IV] In ethene and 1-olefin copolymerization, the reactivity ratios of siloxy-substituted *meso*-isomers are comparable to those of *rac*-Me₂Si[2-Me-Benz[e]Ind]₂ZrCl₂ [107]. Typically, mixtures of racemic isomers are employed, due to the stereo-control in propene polymerization and the higher molecular weight.

The changes in ligand symmetry alter the microstructure of the prepared polymer. Catalysts with C_S-symmetry enable the production of highly syndiotactic polypropene [122]. An example of this is *i*Pr[Cp][Flu]ZrCl₂. Based on the published reactivity ratios, this catalyst has better copolymerization ability than *rac*-Me₂Si[Ind]₂ZrCl₂ [85, 100, 123].

The replacement of one of the cyclopentadienyl ligands with a (*tert*BuN)-ligand has been shown to lead to superior copolymerization properties. A half-metallocene compound, [CpMe₄SiMe₂N(*t*-Bu)]TiCl₂, or CGC, has an extremely good comonomer response as measured by comonomer content in the polymer vs. feed ratio [124]. Even at 140°C, an *r*_E value as low as 8.8 has been determined [24]. The high comonomer response has been attributed to the low steric hindrance at the active site. However, electronic factors lower the activity of this half-metallocene catalyst [125].

6 INFLUENCE OF THE CATALYST AND POLYMERIZATION CONDITIONS ON LONG-CHAIN BRANCHING

Considering LCB formation via the copolymerization route, the vinyl end-group selectivity and comonomer response of the employed catalyst are important factors in determining the polymer structure.

Besides the choice of catalyst, polymerization processing conditions are also likely to have a great role in the formation of LCB. The forming polymer remains in the solution when the polymerization temperature is above the polymer melting point. The polymer precipitates from the solution partly or totally if the polymerization is carried out under slurry conditions, at temperatures below the polymer melting point. When a supported catalyst is used, the forming polymer chains encapsulate the catalyst particles and the polymerization occurs in the polymer phase [126].

The precipitation has a great influence on the mobility of the chains and monomer diffusion rate coefficients, which may account for the LCB formation [32]. Also, the polymer concentration effects the diffusion rate in the slurry polymerization. At high polymer concentration [127-129] the ethene diffusion rate is strongly retarded, which inevitably leads to a decrease in the monomer concentration in solution [130]. This has an enormous influence on the monomer and macromonomer concentration in the vicinity of the active site.

Another important factor is the polymerization reactor operating conditions. In a batch polymerization, the macromonomer concentration increases and the monomer concentration decreases as the polymerization proceeds. The monomer concentration is constant in semi-batch polymerization. Only in the continuous stirred tank reactor system (CSTR), both monomer and macromonomer concentrations are constant after the steady-state conditions are achieved. To control the branching, the last mentioned method appears to be the best way to perform copolymerization reactions [125].

In this work, polymerizations were mainly carried out in slurry using the semibatch method [I-VI, VIII]. A series of solution polymerizations was carried out in a CSTR system [VII]. Monomer, comonomer, and hydrogen concentrations, catalyst choice, and polymerization time influenced LCB as measured with rheological means [III, V, VI]. Utilizing the CSTR system it was observed that the [ethene] / [macromonomer] ratio significantly influenced the LCB content.

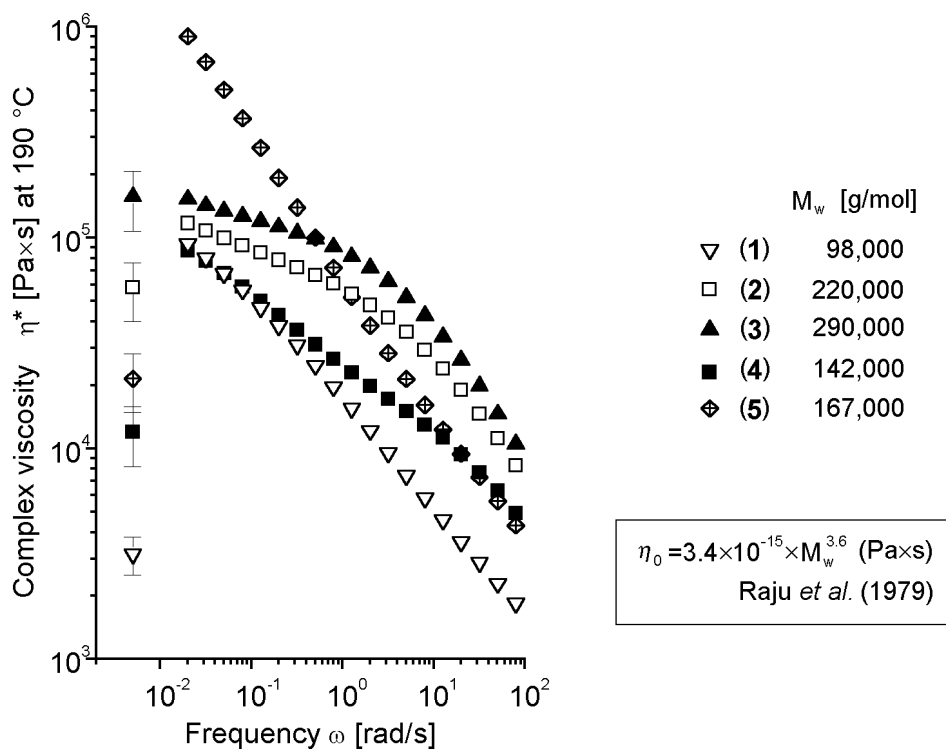


Figure 6.1 Complex viscosity (η^*) curves of polyethenes produced with catalysts **1-5**/MAO under similar polymerization conditions. Single points shown at the left of the graph are calculated zero-shear viscosities (η_0) expected for linear polymers. The measured η^* of polyethenes produced with **2** and **3** approached the calculated η_0 [48], whereas the η^* of other polymers deviated, indicating the presence of long-chain branches [V].

6.1 The effect of the catalyst on branching

Figure 6.1 shows the complex viscosities (η^*) as a function of oscillation frequency (ω) for polyethenes produced with catalysts **1 - 5** under similar polymerization conditions [V]. The samples are the homopolymers reported in Table 4.1. Polyethenes obtained with **1** and **5** are expected to be the most highly branched, as their viscosities at $\omega = 0.02$ rad/s, were 30- and 42-fold higher, respectively, compared to the calculated η_0 values of linear polyethenes of the same M_w .

The increase in the viscosity level was much smaller in polyethenes produced with other catalysts. Polyethylene catalyzed by **4** had a 7-fold and PE obtained from **2** a 2-fold higher viscosity. The η^* of polyethylene catalyzed by **3** was very close to the theoretical value, suggesting the absence of branching [V].

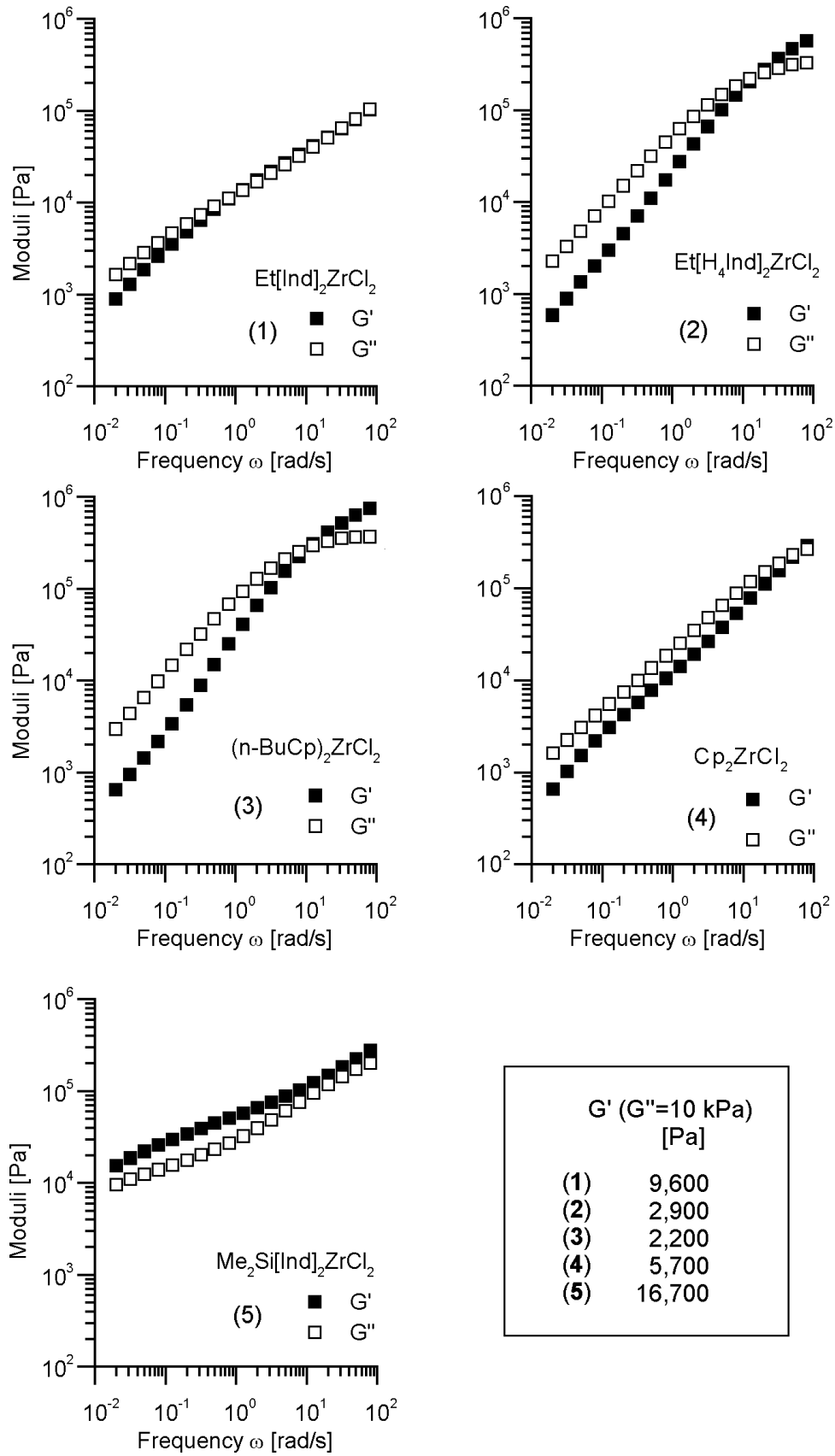


Figure 6.2 Moduli (G' = storage modulus, G'' = loss modulus) curves of polyethylenes produced with catalysts 1-5. Polyethylenes 1 and 5 have greatly elevated G' values due to LCB, whereas the moduli curves of 2 and 3 resemble the moduli curves of linear polymers [V].

Figure 6.2 shows the moduli curves of polyethenes produced with catalysts **1-5**. In addition, a storage modulus (G') value at reference loss modulus value ($G''=10$ kPa) is shown to give a numeric value for the melt elasticity (G' vs. G''). Melt elasticity is a very sensitive tool for detecting differences in the molecular structure, as an increase in the M_w/M_n or even a small LCB content increases the melt elasticity. For linear polymers, the molecular weight does not effect the melt elasticity.

All polymer samples had a narrow M_w/M_n (2.2-2.5). The linear, narrow M_w/M_n polyethenes have in some cases $G'(G''=10$ kPa) values close to 1,000 Pa [**III**, **VI**, **VII**], although due to the high molecular weight tail, values up to 2,500 Pa may be observed. Hence, the observed major differences in the melt elasticity are due to LCB. Different molecular weights complicate the comparison, but in general terms it can be concluded that the polyethene produced with **1** and **5** are more branched than that produced with **4**, which contains more branching than almost linear or linear polymers obtained with **2** and **3**.

The rheological properties are in line with the proposed LCB mechanism, as the differences in the vinyl end-group selectivity (Figure 4.1) and the copolymerization ability (Table 5.1) suggested that **1** and **5** were more suitable catalysts for producing LCB polyethene than **2** or **3**.

The rheological properties of polyethenes produced with siloxy-substituted catalysts **7-10** are collected in Table 6.1 [**IV**]. Those catalysts have an even higher comonomer response (Table 5.2) than **1** or **5**. All samples have very high $\eta^*(\omega_{ref})$ and $G'(G''_{ref})$ values indicating the presence of LCB. Polyethene prepared with **10** contained 0.06 LCB / 1000 C according to a ^{13}C NMR spectroscopic measurement.

The polymerizations with the siloxy-substituted catalysts were carried out at 40°C using 3-fold higher ethene concentration compared to the series carried out with **1-5**. Although it is not possible to perform a direct comparison of the results between these two series, the use of a lower temperature appeared to favor LCB formation. Two factors are considered to contribute: 1) comonomer response is higher at a lower temperature, and 2) polymer precipitation occurs faster at a lower temperature, which changes the mass transfer properties. This may have some importance regarding the LCB formation. This, however, requires further studies.

Table 6.1 Melt rheological properties of polyethenes produced with siloxy-substituted catalysts **7-10** activated with MAO at 40°C. $[C_2H_4] = 0.24$ mol/L **[IV]**.

Catalyst	M_w [kg/mol]	M_w/M_n	Calcd	Measured	
			η_0 [Pa×s] ^a	$\eta^*(0.02$ rad/s) [Pa×s]	$G'(G''=10$ kPa) [Pa]
7	127	2.1	8,000	526,000	9,520
8	190	2.3	34,000	1,220,000	12,500
9	62	2.0	600	18,700	5,960
10	118	2.3	6,200	662,000	10,600

^a The η_0 has been calculated using the equation $\eta_0 = 3.4 \times 10^{-15} \times M_w^{3.6}$ [Pa×s] from ref. [48].

6.2 The effect of ethene concentration

The decrease in the ethene concentration increases LCB content as measured from the change in the rheological behavior shown in Table 6.2 **[III]**. The polymer produced with $C_E = 0.40$ M (short polymerization time) had an E_a and η^* values close to the expected values of linear polymers. These values were dramatically increased in the polyethene produced at the lowest C_E . A small increase in the G' value could be explained with a broadening of M_w/M_n from 2.0 to 3.2. However, high G' values cannot be explained using the difference in the M_w/M_n , but with LCB instead.

Table 6.2 Melt rheological properties of the polyethenes polymerized with **1**/MAO in a semibatch flow reactor at 80°C. A decrease in the C_E increased the branching **[III]**.

$[C_2H_4]$	t_p	M_w	M_w/M_n	Calcd	$\eta^*(0.02$ rad/s)	G' at	E_a
[mol/L]	[min]	[kg/mol]		η_0 [Pa×s] ^a	at 190°C [Pa×s]	$G''(10$ kPa) [Pa]	[kJ/mol]
0.40	10	69	1.9	900	1,540	1,700	29
0.40	25	71	1.9	1,000	3,500	3,200	33
0.24	10	70	2.0	950	2,080	2,300	30
0.08	10	86	2.2	2,000	21,700	6,800	37
0.08	20	98	2.4	3,200	94,000	9,600	42
0.04	25	120	2.8	6,600	185,000	11,500	44
0.02	30	147	3.2	14,000	395,000	13,200	45

^a The η_0 was calculated using equation $\eta_0 = 3.4 \times 10^{-15} \times M_w^{3.6}$ [Pa×s] from ref. [48].

Figure 6.3 shows the η^* vs. ω curves for polyethenes produced at different C_E . Shear thinning is significant for the samples produced at low C_E . The influence of the polymerization time on LCB indicated that the polymer concentration had an influence on the branching probability. Whether this effect was only a pure macromonomer concentration or diffusion effect could not be concluded. In the polymerization system being employed, the diffusion controlled branching is possible if the migration of the polymer chains or chain-end segments is retarded due to increased polymer concentration in the slurry. This would result in an increase in the macromonomer concentration in the vicinity of the active site [III]. It has been suggested that the probability for the macromonomer reincorporation and LCB formation is high enough only before it has drifted away from the vicinity of the active site [23].

The C_E effect for the polymers produced with **2**, **3** and **4** indicated a clear deviation from linearity only at the lowest C_E . The E_a values were comparable to the values expected for linear polyethenes and the differences between theoretical η_0 and measured $\eta^*(0.02 \text{ rad/s})$ values were small. Also, the G' values were lower than those measured for polymers prepared with **1** [III, V].

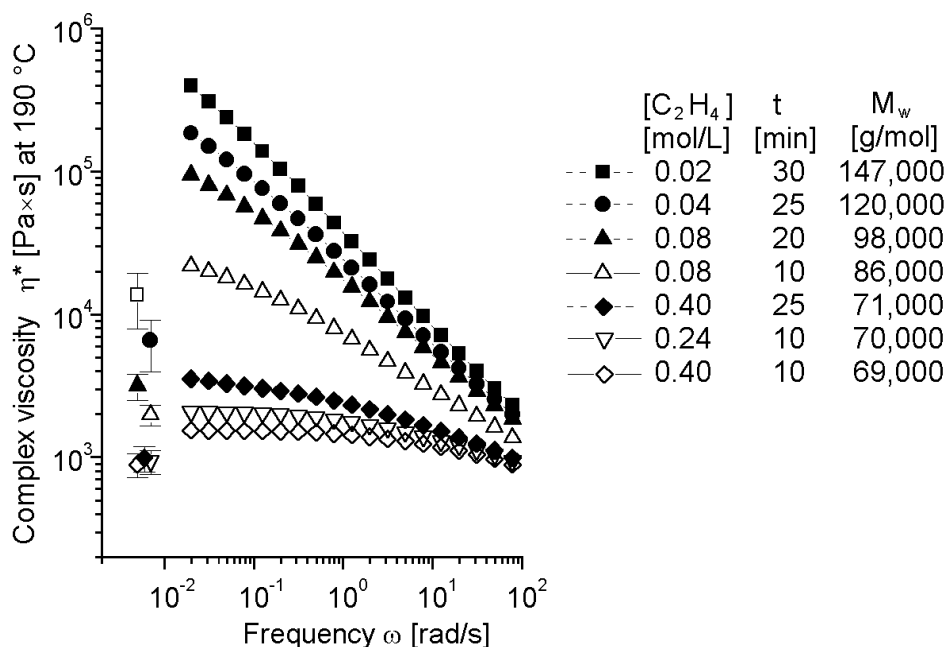


Figure 6.3 Melt rheological behavior of polyethenes polymerized with **1**/MAO varying the ethene concentration and polymerization time. A decrease in the C_E resulted in the strongly elevated η^* at low shear rates and significant shear thinning due to the LCB. Single points shown left in the graph represent theoretical η_0 values [48] expected for a linear polymer. The polymers with high M_w or LCB structure have a true η_0 value that is higher than the measured $\eta^*(0.02 \text{ rad/s})$ value.

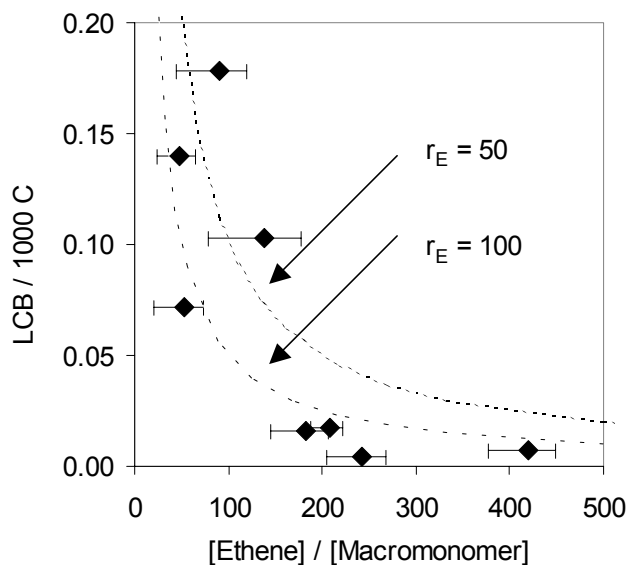


Figure 6.4 The effect of [ethene] / [macromonomer] ratio on the LCB content in **5**/MAO catalyzed polyethenes produced in a CSTR at 140°C. The reactivity of ethene was estimated to be 75-fold higher to that of macromonomer **[VII]**.

Rheological studies showed in a qualitative manner, that the LCB content increases with decreasing ethene concentration. Figure 6.4 shows a quantitative analysis of the ^{13}C NMR based LCB content in polyethene as a function of the [ethene] / [macromonomer] ratio **[VII]**. The LCB content was the highest at low ratios and rapidly decreased with an increase in the ratio. This is in line with the LCB formation via the copolymerization reaction.

Table 6.3 The effect of hydrogen on the melt rheological properties of the polyethenes in a semibatch flow reactor at 80°C **[III, V]**.^a

	[C ₂ H ₄]	H ₂	M _w	M _w /M _n	Calcd	η*(0.02 rad/s)	G' at	E _a
	[mol/L]	feed	[kg/mol]		η ₀	at 190°C	G''(10 kPa)	[kJ/mol]
		[mmol]			[Pa×s] ^b	[Pa×s]	[Pa]	
1	0.24	0.0	70	2.0	900	2080	2,300	30
1	0.24	1.3	59	1.9	500	980	1,800	n.m.
1	0.08	0.0	98	2.4	3,200	94,000	9,600	42
1	0.08	0.5	65	2.1	700	5930	5,400	38
2	0.24	0.4	69	1.9	900	1200	1,200	27

^a **1** = *rac*-Et[Ind]₂ZrCl₂; **2** = *rac*-Et[H₄Ind]₂ZrCl₂; cocatalyst MAO; solvent toluene.

^b The η₀ was calculated using the equation η₀ = 3.4 × 10⁻¹⁵ × M_w^{3.6} (Pa×s) from ref. [48].

6.3 The effect of hydrogen

The introduction of hydrogen suppressed LCB formation. Table 6.3 shows the effect of hydrogen on the melt rheological properties [III]. For the polymer obtained with **1** at $C_E = 0.08$ M, the introduction of hydrogen decreased the E_a value from 42 to 38 kJ/mol, the G' value from 9,600 to 5,400 Pa, and diminished the discrepancy between the theoretical and measured viscosity. The polymer produced without hydrogen at $C_E = 0.24$ M had rheological properties resembling those of linear polymers. Therefore, it was not unexpected that the introduction of hydrogen did not much affect the rheological behavior, except that due to the decrease in the M_w . Polyethylene catalyzed by **2** had a very low G' value (1,200 Pa). The low G' value is attributed to the absence of not only LCB, but also the high M_w tail that can have a marked influence on the melt elasticity.

6.4 The effect of comonomer

Comonomer may be used to suppress or enhance LCB formation [III, VI]. The use of 1-olefins decreases the polymer vinyl bond concentration when chain transfer to the comonomer takes place resulting in vinylidene bond formation. The use of nonconjugated α,ω -dienes, in turn, increases the vinyl bond concentration and LCB formation probability. Moreover, in slurry polymerization, copolymer solubility increases with decreasing crystallinity and melting point, which also accounts for the LCB formation probability. LCB content has also been found to increase with a low 1-olefin content [32, 41, 131], possibly due to the change in mass transfer properties.

The introduction of 1-hexadecene had a similar influence as hydrogen on the rheological properties suppressing LCB. As seen in Table 6.4, the $\eta^*(0.02 \text{ rad/s})$ and G' values were lowered [III]. The E_a value remained almost unchanged. This is a result of a two different effects of the comonomer incorporation: an increase in the comonomer content increases E_a but simultaneously it appears to decrease the LCB content, which lowers the E_a . These opposite effects mask the influence of each other. The $G' = 2,500$ Pa value of **1** catalyzed copolymer, 3.4 mol-% comonomer, suggests a very low LCB content. The E_a and G' values obtained for **3** catalyzed copolymers are considered to represent the properties of linear polymers in which only SCB influences the melt

behavior. The calculated η_0 values are close to the measured values, and the E_a increases slightly as expected for a polymer with SCB. Different methods can be employed to separate the effect of SCB and LCB on the E_a [44,132].

The use of diene as a comonomer, however, has the opposite effect on the branching. This is seen in Table 6.5 [VI]. Rheological properties (η^* , G' , and E_a) are drastically increased with an increasing diene based vinyl bond content, which eventually leads to the crosslinking.

Table 6.4 The effect of comonomer (1-hexadecene) on the melt rheological properties of the polyethenes in a semibatch flow reactor at 80°C [III].^a

	Comonomer Content [mol-%]	Vinyls [C=C/1000 C]	M_w [kg/mol]	M_w/M_n	Calcd η_0 [Pa×s] ^b	$\eta^*(0.02 \text{ rad/s})$ at 190°C [Pa×s]	G' at $G''(10 \text{ kPa})$ [Pa]	E_a TTS ^c [kJ/mol]
1	0.0	0.4	98	2.4	3,200	94,000	9,600	42
1	0.8	0.5	74	2.2	1,200	8,100	4,400	42
1	3.4	0.4	64	2.0	700	1,680	2,500	41
3	0.0	0.1	290	2.3	160,000	152,000	2,200	29
3	0.3	0.1	183	2.0	30,000	28,900	1,200	27
3	1.2	0.1	80	2.0	1,500	2,700	890	33.5

^a **1** = Et[Ind]₂ZrCl₂/MAO; **3** = (*n*-BuCp)₂ZrCl₂/MAO; [C₂H₄] = 0.08 M; solvent toluene

^b Theoretical η_0 was calculated using equation $\eta_0 = 3.4 \times 10^{-15} \times M_w^{3.6}$ (Pa×s) from ref [48].

^c TTS = time-temperature superposition.

Table 6.5 The effect of comonomer (1,5-hexadiene) on the melt rheological properties of the polyethenes in a semibatch flow reactor at 80°C [VI].^a

1,5-HD Content [mol-%]	Vinyls [C=C / 1000 C]	M_w [kg/mol]	M_w/M_n	Calcd η_0 [Pa×s] ^b	$\eta^*(0.02 \text{ rad/s})$ at 190°C [Pa×s]	G' at $G''(10 \text{ kPa})$ [Pa]	E_a $G^*(10 \text{ kPa})$ [kJ/mol]
0.0	0.4	77	2.2	1,300	3,200	3,360	31
1.2	0.9	83	2.2	1,700	70,400	8,470	45
1.5	1.3	93	2.6	2,600	78,600	8,640	
1.8	1.5	98	2.6	3,200	155,000	9,840	55
2.9	1.9	113	3.2	5,300	741,000	13,860	
3.8	2.2	188	4.7	33,000	n.d.	n.d.	

^a catalyst Et[Ind]₂ZrCl₂/MAO; [C₂H₄] = 0.08 M; solvent toluene.

^b Calculated using equation $\eta_0 = 3.4 \times 10^{-15} \times M_w^{3.6}$ (Pa×s) from ref [48].

n.d. = not determined due to the extremely slow relaxation.

To further test the importance of vinyl bond content and copolymerization ability in LCB formation, a polymerization series with two catalysts having very different comonomer response – with low inherent vinyl bond formation tendency and very facile hydrogen reactivity – was carried out [VI]. The polymerization results are summarized in Table 6.6. The ethene concentration was kept high to avoid inherent LCB formation.

Copolymers produced with a poor copolymerization catalyst **3** were linear or contained only a very small amount of LCB. The homopolymer that contained very few vinyl bonds was concluded to be very linear based on its rheological properties. The copolymer with 1.5 C=C / 1000 C had slightly elevated η^* vs. η_0 , G' , and E_a values. These values suggest the presence of a small amount of branching. The M_w/M_n was broadened to the value of 8.8 only when a copolymer was produced at low ethene concentration, which suggested that excessive branching took place only under very specific polymerization conditions.

Very different polymer properties were observed with a good copolymerization catalyst **6**. The copolymers had drastically modified rheological properties at very low comonomer content. Slightly higher comonomer feed resulted in the formation of a crosslinked polymer that was difficult to remove from the reactor due to gel formation.

Table 6.6 Catalyst and vinyl bond content effect on the melt rheological properties of the polyethenes in a semibatch flow reactor at 80°C [VI].^a

	1,7-OD Content [mol-%]	Vinyls [C=C / 1000 C]	M_w [kg/mol]	M_w/M_n	Calcd η_0 [Pa×s] ^b	$\eta^*(0.02 \text{ rad/s})$ at 190°C [Pa×s]	G' at $G''(10 \text{ kPa})$ [Pa]	E_a $G^*(10 \text{ kPa})$ [kJ/mol]
3	0.00	<0.1	77	2.2	1,300	1,410	1,060	27
3	0.15	0.7	63	1.8	640	740	1,000	
3	0.16	1.1	74	1.9	1,150	1,370	2,000	
3	0.27	1.5	65	1.9	720	2,270	2,240	33
6	0.00	<0.1	146	2.4	13,300	39,400	3,870	28
6	0.17	0.4	101	2.5	3,500	170,000	10,460	57
6	0.23	0.5	68	2.3	850	11,300	6,200	43

^a **3** = (n-BuCp)₂ZrCl₂/MAO; **6** = Et[Ind]₂HfCl₂/MAO; [C₂H₄] = 0.40 M; comonomer 1,7-octadiene; solvent toluene.

^b Calculated using equation $\eta_0 = 3.4 \times 10^{-15} \times M_w^{3.6}$ (Pa×s) from ref [48].

7 CORRELATION OF RHEOLOGICAL PROPERTIES WITH POLYMER STRUCTURE

Three different basic methods are used for the detection of LCB; ^{13}C NMR spectroscopy [9, 133], gel permeation chromatography [134, 135], and rheological measurements [49, 52]. Melt rheological measurements are the most sensitive methods for detecting very low concentrations of LCB. However, the analysis of LCB is achieved best with a combination of all three methods.

The LCB density in single-center polyethenes is typically in the range of 0.01 – 0.2 branch points per 1000 main chain carbons [39, 42, 46, **VII**, **VIII**]. In many cases, low LCB content is difficult to detect with ^{13}C NMR spectroscopic or multi-detector GPC methods [46]. In addition, the ^{13}C NMR technique is short-handed, as it cannot differentiate C_6 branches from the longer ones. Nevertheless, ^{13}C NMR spectroscopy has been considered to be the only method to prove the existence of LCB in polyethene.

For the polymers with very low levels of LCB, the rheological methods appear to be most pragmatic [10, 38, 40, 43, 46]. However, the information from melt rheological measurements is indirect; the measured rheological properties result from the combined effects of the molecular weight and distribution as well as branch length, content, and distribution. Recently, a lot of research has been conducted in this field, both from the theoretical [47, 136] and experimental [37-46, 137, 138] point of view.

The LCB in polyethene observed in rheological analysis was compared to the results obtained in microstructural analysis by ^{13}C NMR spectroscopy and GPC [**VII**, **VIII**]. In addition, a comparison between the different analytical methods – GPC, ^{13}C NMR, and FTIR spectroscopy – was performed.

Figure 7.1 shows a comparison between the GPC based M_w and the measured η_0 or $\eta^*(\omega=0.01 \text{ s}^{-1})$ values [**VIII**]. The η_0 of linear polyethenes has been found to follow the correlation described in Fig. 7.1 (the solid line). The η_0 of a linear reference polyethene sample (IUPAC 5A) followed this relationship. Due to LCB, the η_0 or $\eta^*(\omega=0.01 \text{ s}^{-1})$ values of the six samples are up to 50-fold higher than compared to the expected values for linear polymers. A comparison with the LCB values obtained in ^{13}C NMR measurements revealed that even the samples with barely detectable amounts of LCB have clearly elevated viscosity levels.

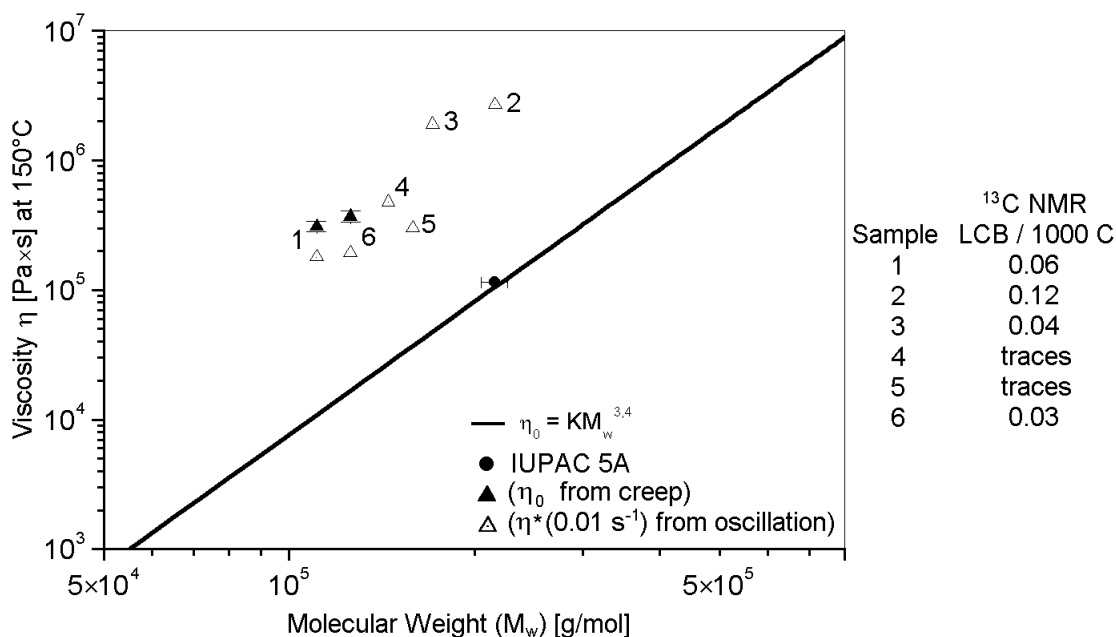


Figure 7.1 The molecular weight dependence of the η_0 or $\eta^*(\omega=0.01 \text{ s}^{-1})$ of linear and long-chain branched polyethylenes. Samples 1 and 2 were prepared with *rac*-Et[Ind]₂ZrCl₂/MAO; 3 and 4 with *rac*-Me₂Si[Ind]₂ZrCl₂/MAO; and 5 and 6 with *rac*-Et[H₄Ind]₂ZrCl₂/MAO. The filled symbols denote the η_0 determined from creep experiments, the open symbols η^* from dynamic analysis at an $\omega=0.01 \text{ s}^{-1}$. A discrepancy from the solid line indicates the presence of branching [VIII].

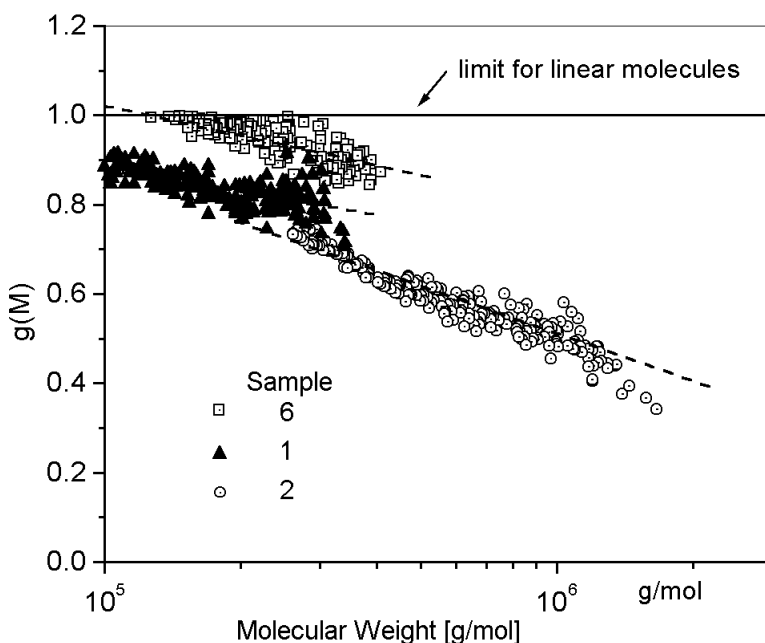


Figure 7.2 The contraction factor $g(M)$ as a function of molecular weight of long-chain branched samples measured with a GPC-MALLS system. The lower $g(M)$ value indicates a greater amount of branching [VIII]. The samples are the same as in Fig. 7.1.

Figure 7.2 shows a comparison of contraction factors, g , as a function of the molecular weight of selected homopolyethene samples. Branched molecules have a smaller radius of gyration than linear polymers, which results in g values less than one [VII]. The value of g correlated well with the ^{13}C NMR based branching level. (see Fig. 7.1) A decrease in the g value with the increasing M_w indicated an increased fraction of branched chains at the high M_w . The high M_w chains are more likely to contain two or more branches in a chain, which may account for the observed rheological properties.

The characterization results for polyethenes prepared in a CSTR system are collected in Table 7.1 [VII]. Figure 7.3 shows the measured η_0 vs. calculated η_0 values. Regarding branch distribution, the CSTR system may offer better control than the semibatch slurry system over the polymer structure. The rheological properties and ^{13}C NMR based LCB content correlated well, as η_0 , (G' vs. G'') and E_a increased with the branch content. Due to the low M_w , these polymers overall had much lower G' and E_a values than the polymers produced in slurry systems. Also, the increase in the viscosity level was less pronounced. (Fig. 7.3) The measured η_0 was only up to 4-fold higher compared to the η_0 of linear polyethenes of the same M_w . Based on the polymerization conditions employed, (Fig. 6.4) sample 1 is assumed to have a very linear structure whereas samples 6 and 8 are expected to contain more LCB than the other samples. The measured polymer properties are in line with this assumption [VII].

Table 7.1 Molecular structure and rheological properties of polyethenes produced with *rac*-Me₂Si[Ind]₂ZrCl₂/MAO in a CSTR reactor at 140°C [VII].^a

Sample	M_w (kg/mol)	M_n (kg/mol)	LCB / 1000 C	$G'(G''_{ref})$ [Pa]	$E_{a,0}$ [kJ/mol]	E_{a,G^*ref} [kJ/mol]
1	55	25	0.00	1,210	29.4	29.1
2	53	21	0.01	1,820	30.8	29.7
3	52	24	0.02	2,270	33.0	29.5
4	53	24	0.00	1,940	31.2	29.7
5	44	19	0.07	3,000	38.7	35.5
6	36	16	0.18	3,170	43.6	42.0
7	37	16	0.10	3,100	36.2	35.6
8	49	19	0.14	4,810	49.5	47.0
9	58	26	0.02	2,450	33.1	30.1

^a $G''_{ref} = 10$ kPa. $E_{a,0}$ was calculated from the η_0 and $E_{a,1}$ from the $\eta^*(G^*=10$ kPa) values.

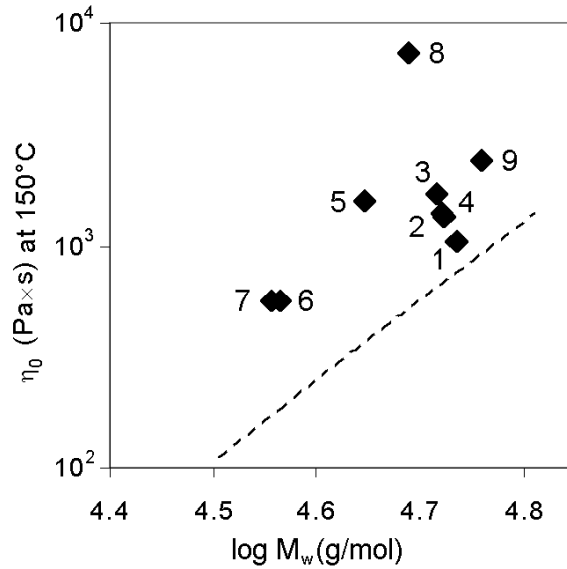


Figure 7.3 Correlation between the M_w and zero-shear viscosity (η_0) of polyethenes prepared in a CSTR. The straight line represents the $\eta_0 - M_w$ relationship of linear polyethenes using the equation $\eta_0 = 6.8 \times 10^{-15} \times M_w^{3.6}$ [44]. See Table 7.1 for the characterization details of samples 1-9.

Figures 7.1 and 7.3 can qualitatively indicate whether a polymer is branched or linear. In order to find a quantitative correlation between the rheological properties, M_w , and LCB content, an experimental relationship between the branch length, content and molecular weight was used [44]. Equation 7.1 describes this relationship, in which the flow activation energy of the branched polymer ($E_{a,B}$) is composed of the flow activation energy of a linear polymer ($E_{a,L}$) and the activation energy increase due to branched chains ($\Lambda \times \phi M_A / M_E$).

$$E_{a,B} = E_{a,L} + \Lambda \times \phi \frac{M_A}{M_E} \quad (7.1)$$

M_A is the molecular weight of the arm, which is assumed to be equal to M_w . M_E is the entanglement molecular weight of polyethene (1250 g/mol). Λ is the activation coefficient and ϕ is the volume fraction of branched polymer as described in Equation 7.2. The molecular weight of the repeat unit ($-\text{CH}_2-$) is 14 g/mol.

$$\phi = M_w \times \frac{LCB / 1000 C}{1000 \times M_{\text{repeat unit}}} \quad (7.2)$$

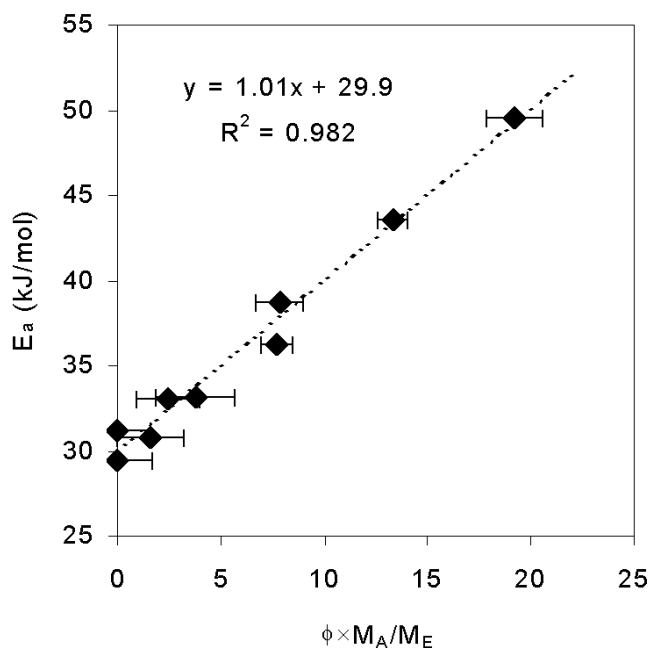


Figure 7.4 The influence of long-chain branch content and arm length on the flow activation energy E_a . The coefficients for Eq. 7.2 are obtained from the slope; $\Lambda = 1.01$ kJ/mol; and the intersection; $(E_a)_L = 29.9$ kJ/mol [VII].

Figure 7.4 shows the correlation between the experimentally determined $E_{a,0}$, M_w , and LCB content. The correlation coefficient R^2 showed a very good agreement. The value of Λ was essentially the same as reported for a series of hydrogenated polybutadienes and ethene–1-octene copolymers, but there was a contradiction between the Λ values obtained for a series of homopolyethenes produced with CGC [44]. It has been suggested that the difference is due to differences in the branch structure [46, 139]. The $E_{a,L}$ value was 10% higher than the reported values.

This method appears to be very useful in comparing the rheological properties and molecular structure of polyethene. Equation 7.2 may prove very useful in determining polymer structure from the rheological analysis. However, the successful utilization is challenging, as the equation is very sensitive to the accuracy of the measured LCB content. The accuracy of ^{13}C NMR based measurement of LCB content is limited, which may lead to dramatic errors for the high M_w polyethenes. Another problem in high M_w polyethenes arises from the difficulty in obtaining the η_0 values for the subsequent determination of $E_{a,0}$.

7.1 Correlation between the analytical methods.

In order to generally test the accuracy and reliability of the results, a comparison of different analysis methods was carried out. Figure 7.5 shows the vinyl bond content ($C=C / 1000 C$) of polyethenes determined with FTIR and ^{13}C NMR spectrometers and polymerization degrees (X_n) measured with GPC and the ^{13}C NMR spectrometer.

In vinyl bond analysis with FTIR spectrometer, the $C=C / 1000 C$ content was calculated from Equation 7.3. The value of the molar coefficient factor (ε) was 1.087, (A) was the height of the 908 cm^{-1} absorption peak, and (b) the thickness of the sample (mm). The ^{13}C NMR result was based on the area of allyl peak at 33.9 ppm divided by the areas of other peaks in the aliphatic region.

$$C=C / 1000 C = \frac{A}{\varepsilon \times b} \quad (7.3)$$

The X_n from the refractometer equipped GPC results was based on the M_n values and the X_n from ^{13}C NMR measurements was obtained by comparing the sums of areas of α -carbon peaks of vinyls (33.9 ppm) and saturated end-group peaks (32.2, 22.9, and 14.1 ppm) to the total areas of peaks in the aliphatic region. ^{13}C NMR results were corrected for branching. R^2 values indicate very good correlation between the analytical methods.

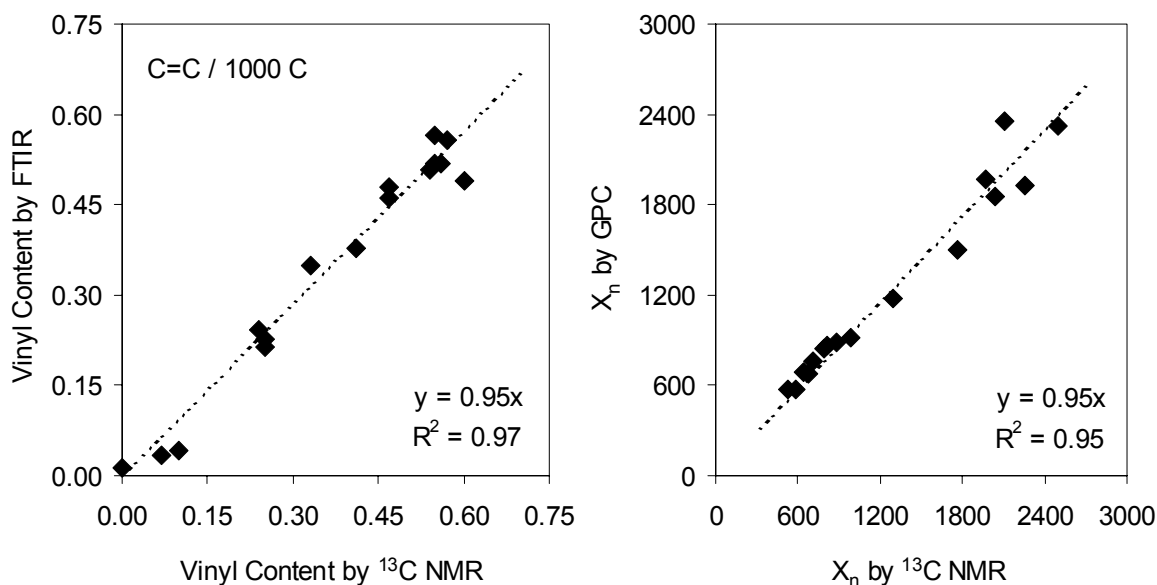


Figure 7.5 Comparison of FTIR and ^{13}C NMR based vinyl contents ($C=C / 1000 C$) and GPC and ^{13}C NMR based number average polymerization degrees (X_n) [VII, VIII].

8 SUMMARY

In this thesis the polymerization behavior of known (**1-6**) and novel siloxy-substituted (**7-10**) metallocene catalysts activated with methylaluminoxane was studied. Features of the polymer structure like molecular weight, end-group types, comonomer, and long-chain branch content are strongly dependent on catalyst and polymerization conditions employed.

Long-chain branching in polyethene could be detected with a ^{13}C NMR spectrometer, light-scattering detector GPC, and melt rheological measurements. The metallocene catalyzed polyethenes contained up to 0.2 LCB / 1000 C [**I**, **IV**, **VII**, **VIII**]. Long-chain branched polymers exhibited modified rheological properties – increased complex viscosity (η^*) at low shear rate, enhanced melt elasticity (G' vs. G''), and elevated flow activation energy (E_a) – when compared to linear polyethenes [**I**, **III-VIII**]. The sensitivity of melt rheological measurements was superior to other characterization methods in detecting small amounts of long-chain branching. The rheological properties measured correlated well with the ^{13}C NMR based polymer structure [**VII**, **VIII**].

Of all catalysts studied, bis(indenyl) *ansa*-metallocenes are the best candidates for the production of LCB polyethene [**II-V**]. The results obtained support the view that long-chain branching in metallocene catalyzed ethene polymerization takes place via a copolymerization reaction: A vinyl terminated polyethene chain is incorporated into a growing chain. The vinyl end-group selectivity and copolymerization ability of metallocene/MAO catalyst system is strongly dependent on the metallocene ligand structure. Some catalysts were found to have an almost 100% selectivity towards vinyl terminations and relatively good copolymerization abilities.

Besides the catalyst choice [**III-V**], the polymerization conditions have a dramatic effect on the long-chain branch content in polyethenes [**II-VI**]. The amount of branching is increased by decreasing the ethene concentration [**III**, **V**, **VII**], or increasing the amount of unsaturations in the polymer chain via diene addition [**VI**]. The introduction of hydrogen, in turn, decreases branching [**III**]. These parameters may fully or partially compensate differences given by catalyst structures. Moreover, polymerization process conditions may have a significant role in the long-chain branch formation process via mass-transfer effects.

REFERENCES

1. Todd, M., Polyolefins go global, *Eur. Chem. News* 22-28 Oct (2001), 20-22.
2. Ittel, S. D., Johnson, L. K., Brookhart, M., Late-metal catalysts for ethylene homo- and copolymerization, *Chem. Rev.* **100** (2000) 1169-1203.
3. Alt, H. G., Köppl, A., Effect of the nature of metallocene complexes of group IV metals on their performance in catalytic ethylene and propylene polymerization, *Chem. Rev.* **100** (2000) 1205-1221.
4. Coates, G. W., Precise control of polyolefin stereochemistry using single-site metal catalysts, *Chem. Rev.* **100** (2000) 1223-1252.
5. Resconi, L., Cavallo, L., Fait, A., Piemontesi, F., Selectivity in propene polymerization with metallocene catalysts, *Chem. Rev.* **100** (2000) 1253-1345.
6. Imanishi, Y., Naga, N., Recent developments in olefin polymerizations with transition metal catalysts, *Prog. Polym. Sci.* **26** (2001) 1147-1198.
7. Santamaría, A., Influence of long chain branching in melt rheology and processing of low density polyethylene, *Mater. Chem. Phys.* **12** (1985) 1-28.
8. Doak, K. W., Ethylene polymers. In *Encyclopedia of Polymer Science and Engineering*, eds. H. F. Mark, N. M. Bikales, C. G. Overberger, G. Menges, 2. Ed., vol 6, John Wiley & Sons, New York 1985, pp. 383-494.
9. Randall, J. C., Characterization of long-chain branching in polyethylenes using high-field carbon-13 NMR, in *Polymer characterization by ESR and NMR*, eds. A. E. Woodward and F. A. Bowey, ACS Symposium series, vol. 142, American Chemical Society, Washington, USA 1980, pp. 93-118.
10. a) Shroff, R. N., Mavridis, H., Long-chain-branching index for essentially linear polyethylenes, *Macromolecules* **32** (1999) 8454-8464. b) Shroff, R. N., Mavridis, H. *ibid.* 8696.
11. Reinking, M. K., Orf, G., McFaddin, D., Novel mechanism for the formation of long-chain branching in polyethylene, *J. Polym. Sci. Part A: Polym. Chem.* **36** (1998) 2889-2898.
12. Whitte, W. H., Randall, J. C., Leigh, C. H., On the contribution of long chain branching to polyethylene melt rheology, *Chem. Eng. Commun.* **24** (1983) 139-146.
13. Dickie, B. D., Koopmans, R. J., Long-chain branching determination in irradiated linear low-density polyethylene, *J. Polym. Sci. Part C: Polym. Lett.* **28** (1990) 193-198.
14. Bersted, B. H., On the effects of very low levels of long chain branching on rheological behavior in polyethylene, *J. Appl. Polym. Sci.* **30** (1985) 3751-3765.
15. Harrell, E. R., Nakajima, N., Modified Cole-Cole plot based on viscoelastic properties for characterizing molecular architecture of elastomers, *J. Appl. Polym. Sci.* **29** (1984) 995-1010.
16. Hughes, J. K., Analysis of long chain branching in high density polyethene, *Proceedings Annu. Tech. Conf.*, Soc. Plast. Eng. 1983, pp. 306-309.
17. Moss, S., Zweifel, H., Degradation and stabilization of high density polyethylene during multiple extrusions, *Polym. Degrad. Stab.* **25** (1989) 217-245.

18. Foster, G. N., Wasserman, S. H., Yacka, D. J., Oxidation behavior and stabilization of metallocene and other polyolefins, *Angew. Makromol. Chem.* **252** (1997) 11-32.
19. Brant, P., Canich, J. A. M., Dias, A. J., Bamberger, R. L., Licciardi, G. F., Henrichs, P. M., Long chain branched polymers and a process to make long chain branched polymers, *Int. Pat. Appl. WO 94/07930*, 24 April 1994.
20. Sugawara, M., Branching structure and performances of metallocene-based copolymers, *Proceedings SPO'94*, Schotland Business Reseach, Houston TX, Oct. 1994, pp. 39-50.
21. a) Hamielec, A. E., Soares, J. B. P., Polymerization reaction engineering - metallocene catalysts, *Prog. Polym. Sci.* **21** (1996) 651-706. b) Hamielec, A. E., Soares, J. B. P., Metallocene catalysts and long-chain branching, *Proceedings SPO'96*, Schotland Business Reseach, Houston TX, Oct. 1996, pp. 95-115.
22. Beigzadeh, D., Soares, J. B. P., Hamielec, A. E., Study of long-chain branching in ethylene polymerization, *Polym. React. Eng.* **5** (1997) 141-180.
23. Woo, T. K., Margl, P. M., Ziegler, T., Blöchl, P. E., Static and ab initio molecular dynamics study of the titanium(IV)-constrained geometry catalyst (CpSiH₂NH)Ti-R⁺. 2. Chain termination and long chain branching, *Organometallics* **16** (1997) 3454-3468.
24. Wang, W.-J. Yan, D., Zhu, S., Hamielec, A. E., Kinetics of long chain branching in continuous solution polymerization of ethylene using constrained geometry metallocene, *Macromolecules* **31** (1998) 8677-8683.
25. Soga, K., Uozumi, T., Nakamura, S., Toneri, T., Teranishi, T., Sano, T., Arai, T., Structures of polyethylene and copolymers of ethylene with 1-octene and oligoethylene produced with Cp₂ZrCl₂ and [(C₅Me₄)SiMe₂N(t-Bu)]TiCl₂ catalysts, *Macromol. Chem. Phys* **197** (1996) 4237-4251.
26. Pietikäinen, P. Väänänen, T., Seppälä, J. V., Copolymerization of ethylene and non-conjugated dienes with Cp₂ZrCl₂/MAO catalyst system, *Eur. Polym. J.* **24** (1999) 1047-1055.
27. Pietikäinen, P. Starck, P., Seppälä, J. V., Characterization of comonomer distributions in ethylene / diene copolymers by ¹³C-NMR, and using the segregation fractionation technique by DSC and DMTA, *J. Polym. Sci. Part A: Polym. Chem.* **37** (1999) 2379-2389.
28. Lai, S.-Y., Wilson, J. R., Knight, G. W., Stevens, J. C., Chum, P.-W. S., Elastic substantially linear olefin polymers, *U.S. Patent 5,272,236*, Dec. 21, 1993.
29. Kim, Y. S., Chung, C. I., Lai, S. Y., Hyun, K. S., Melt rheological and thermodynamic properties of polyethylene homopolymers and poly(ethylene/a-olefin) copolymers with respect to molecular composition and structure, *J. Appl. Polym. Sci.* **59** (1996) 125-137.
30. a) Vega, J. F., Muñoz-Escalona, A., Santamaría, A., Muñoz, M. E., Lafuente, P., Comparison of the rheological properties of metallocene-catalyzed and conventional high-density polyethylenes, *Macromolecules* **29** (1996) 960-965. b) Carella, J. M., Comments on the paper "Comparison of the rheological properties of metallocene-catalyzed and conventional high-density polyethylenes" *Macromolecules* **29** (1996) 8280-8281.
31. Howard, P., Maddox, P. J., Partington, S. R., Polymerisation process and polyolefins obtained thereby, *Eur. Pat. Appl. 0 676 421 A1*, 11.10.1995.

32. Harrison, D., Coulter, I. M., Wang, S., Nistala, S., Kuntz, B. A., Pigeon, M., Tian, J., Collins, S., Olefin polymerization using supported metallocene catalysts: development of high activity catalysts for use in slurry and gas phase ethylene polymerizations, *J. Mol. Catal. A: Chem.* **128** (1998) 65-77.
33. Kolodka, E., Wang, W.-J., Charpentier, P. A., Zhu, S., Hamielec, A. E., Long-chain branching in slurry polymerization of ethylene with zirconocene dichloride/modified methylaluminoxane, *Polymer* **41** (2000) 2985-3991.
34. Dealy, J. M., Wissbrun, K. F., *Melt Rheology and its Role in Plastics Processing: Theory and Applications*, Van Nostrand Reinhold, New York 1990, 665 pp.
35. Macosko, C. W., *Rheology: Principles, Measurements, and Applications*, Wiley-VCH, USA 1994, 550 pp.
36. Laun, H. M., Orientation of macromolecules and elastic deformations in polymer melts. Influence of molecular structure on the reptation of molecules, *Prog. Coll. Polym. Sci.* **75** (1987) 111-139.
37. Gahleitner, M., Melt rheology of polyolefins, *Prog. Polym. Sci.* **26** (2001) 895-944.
38. Vega, J. F., Santamaría, A., Muñoz-Escalona, A., Lafuente, P., Small-amplitude oscillatory shear flow measurements as a tool to detect very low amounts of long chain branching in polyethylenes, *Macromolecules* **31** (1998) 3639-367.
39. Yan, D., Wang, W.-J., Zhu, S., Effect of long chain branching on rheological properties of metallocene polyethylene, *Polymer* **40** (1999) 1737-1744.
40. Vega, J. F., Fernández, M., Santamaría, A., Muñoz-Escalona, A., Lafuente, P., Rheological criteria to characterize metallocene catalyzed polyethylenes, *Macromol. Chem. Phys.* **200** (1999) 2257-2268.
41. Malmberg, A., Liimatta, J., Lehtinen, A., Löfgren, B., Characteristics of long chain branching in ethene polymerization with single site catalysts, *Macromolecules* **32** (1999) 6687-6696.
42. Wood-Adams, P. M., Dealy, J. M., Using rheological data to determine the branching level in metallocene polyethylenes, *Macromolecules* **33** (2000) 7481-7488.
43. Wood-Adams, P. M., Dealy, J. M., deGroot, A. W., Redwine, O. D., Effect of molecular structure on the linear viscoelastic behavior of polyethylene, *Macromolecules* **33** (2000) 7489-7499.
44. Wood-Adams, P. M., Costeux, S., Thermorheological behavior of polyethylene: effects of microstructure and long chain branching, *Macromolecules* **34** (2001) 6281-6290.
45. Read, D. J., McLeish, T. C. B., Molecular rheology and statistics of long chain branched metallocene-catalyzed polyolefins, *Macromolecules* **34** (2001) 1928-1945.
46. Shroff, R. N., Mavridis, H., assessment of NMR and rheology for the characterization of LCB in essentially linear polyethylenes, *Macromolecules* **34** (2001) 7362-7367.
47. Janzen, J., Colby, R. H., Diagnosing long-chain branching in polyethylenes, *J. Mol. Struct.* **485-486** (1999) 569-584.
48. Raju, V. R., Smith, G. G., Marin, G., Knox, J. R., Graessley, W. W., Properties of amorphous and crystallizable hydrocarbon polymers. I. Melt rheology of fractions of linear polyethylene, *J. Polym. Sci.: Polym. Phys. Ed.* **17** (1979) 1183-1195.

49. Graessley, W. W., Effect of long branches on the flow properties of polymers, *Acc. Chem. Res.* **10** (1977) 332-339.
50. Bersted, B. H., Slee, J. D., Richter, C. A., Prediction of rheological behavior of branched polyethylene from molecular structure, *J. Appl. Polym. Sci.* **26** (1981) 1001-1014.
51. Carella, J. M., Gotro, J. T., Graessley, W. W., Thermorheological effects of long-chain branching in entangled polymer melts, *Macromolecules* **19** (1986) 659-667.
52. Mavridis, H., Shroff, R. N., Temperature dependence of polyolefin melt rheology, *Polym. Eng. Sci.* **32** (1992) 1778-1791.
53. Wasserman, S. H., Graessley, W. W., Prediction of linear viscoelastic response for entangled polyolefin melts from molecular weight distribution, *Polym. Eng. Sci.* **36** (1996) 852-861.
54. Kalyon, D. M., Yu, D.-W., Moy, F. H., Rheology and processing of linear low density polyethylene resins as affected by alpha-olefin comonomers, *Polym. Eng. Sci.* **28** (1988) 1542-1550.
55. Jacovic, M. S., Pollock, D., Porter, R. S., A rheological study of long branching in polyethylene by blending, *J. Appl. Polym. Sci.* **23** (1979) 517-527.
56. Han, C. D., Villamizar, C. A., Effects of molecular weight distribution and long-chain branching on the viscoelastic properties of high- and low-density polyethylene melts, *J. Appl. Polym. Sci.* **22** (1978) 1677-1700.
57. Han, C. D., Jhon, M.S., Correlations of the first normal stress difference with shear stress and of the storage modulus with loss modulus for homopolymers, *J. Appl. Polym. Sci.* **32** (1986) 3809-3840.
58. Chen, E. Y.-X., Marks T. J., Cocatalysts for metal-catalyzed olefin polymerization: activators, activation processes, and structure-activity relationships, *Chem. Rev.* **100** (2000) 1391-1434.
59. Pédeutour, J.-N., Radhakrishnan K., Cramail, H., Deffieux, A., Reactivity of metallocene catalysts for olefin polymerization: influence of activator nature and structure, *Macromol. Rapid Commun.* **22** (2001) 1095-1123.
60. Cossee, P., Ziegler-Natta catalysis I. Mechanism of polymerization of α -olefins with Ziegler-Natta catalysts, *J. Catal.* **3** (1964) 80-88.
61. Arlman, E. J., Cossee, P., Ziegler-Natta catalysis III. Stereospecific polymerization of propene with the catalyst system $\text{TiCl}_3\text{-AlEt}_3$, *J. Catal.* **3** (1964) 99-104.
62. Grubbs, R. H., Coates, G. W., α -Agostic interactions and olefin insertion in metallocene polymerization catalysts, *Acc. Chem. Res.* **29** (1996) 85-93.
63. Fink, G., Herfert, N., Montag, P., The relationship between kinetics and mechanisms. In *Ziegler Catalysts*, eds. G. Fink, R. Mülhaupt, H.-H. Brintzinger, Springer-Verlag, Berlin Heidelberg 1995, pp. 159-179.
64. Wester, T. S., Johnsen, H., Kittilsen, P., Rytter, E., The effect of temperature on the polymerization of propene with dimethylsilyl bis(1-indenyl) zirconium dichloride / methylaluminoxane and dimethylsilyl bis(2-methyl-1-indenyl) zirconium dichloride / methylaluminoxane. Modeling of kinetics, *Macromol. Chem. Phys.* **199** (1998) 1989-2004.

65. Nele, M., Mohammed, M., Xin, S., Collins, S., Dias, M., Pinto, J. C., Two-state models for propylene polymerization using metallocene catalysts. 2. Application to ansa-metallocene catalyst systems, *Macromolecules* **34** (2001) 3830-3841.
66. Busico, V., Cipullo, R., Cutillo, F., Vacatello, M., Metallocene-catalyzed propene polymerization: from microstructure to kinetics. 1. C_2 -symmetric ansa-metallocenes and the "trigger" hypothesis, *Macromolecules* **35** (2002) 349-354.
67. Sinn, H., Kaminsky, W., Ziegler-Natta catalysis, *Adv. Organomet. Chem.* **18** (1980) 99-149.
68. Tsutsui, T., Mizuno, A., Kashiwa, N., The microstructure of propylene homo- and copolymers obtained with a Cp_2ZrCl_2 and methylaluminoxane system, *Polymer* **30** (1989) 428-431.
69. Siedle, A. R., Lamanna, W. M., Newmark, R. A., Schroeffer, J. N., Mechanism of olefin polymerization by a soluble zirconium catalyst, *J. Mol. Catal. A: Chem.* **28** (1998) 257-271.
70. a) Resconi, L., Piemontesi, F., Franciscano, G., Abis, L., Fiorani, T., Olefin polymerization at bis (pentamethylcyclopentadienyl) zirconium and -hafnium centers: chain-transfer mechanisms, *J. Am. Chem. Soc.* **114** (1992) 1025-1032. b) Resconi, L., Camurati, I., Sudmeijer, O., Chain transfer reactions in propylene polymerization with zirconocene catalysts, *Topics Catal.* **7** (1999) 145-163.
71. Naga, N., Mizunuma, K., Chain transfer reaction by trialkylaluminum (AlR_3) in the stereospecific polymerization of propylene with metallocene $AlR_3 / PhCB(C_6F_5)_4$, *Polymer* **39** (1998) 5059-5067.
72. Shiono, T., Soga, K., Synthesis of terminally aluminum-functionalized polypropylene, *Macromolecules* **25** (1992) 3356-3361.
73. Kissin, Y. V., Brandolini, A. J., Ethylene polymerization reactions with Ziegler-Natta catalysts. II. Ethylene polymerization reactions in the presence of deuterium, *J. Polym. Sci. Part A: Polym. Chem.* **37** (1999) 4274-4280.
74. Tsutsui, T., Kashiwa, N., Mizuno, A., Effect of hydrogen on propene polymerization with ethylenebis(1-indenyl)zirconium dichloride and methylaluminoxane catalyst system, *Makromol. Chem., Rapid Commun.* **11** (1990) 565-570.
75. Carvill, A., Tritto, I., Locatelli, P., Sacchi, M. C., Polymer microstructure as a probe into hydrogen activation effect in ansa-zirconocene / methylaluminoxane catalyzed propene polymerizations, *Macromolecules* **30** (1997) 7056-7062.
76. Kaminsky, W., Lüker, H., Influence of hydrogen on the polymerization of ethylene with the homogeneous Ziegler system bis(cyclopentadienyl) zirconium dichloride / aluminoxane, *Makromol. Chem., Rapid Commun.* **5** (1984) 225-228.
77. Schneider, M. J., Mülhaupt, R., Influence of indenyl ligand substitution pattern on metallocene-catalyzed propene copolymerization with 1-octene, *Macromol. Chem. Phys.* **198** (1997) 1121-1129.
78. Busico, V., Cipullo, R., Chadwick, J. C., Modder, J. F., Sudmeijer, O., Effects of regiochemical and stereochemical errors on the course of isotactic propene polyinsertion promoted by homogeneous Ziegler-Natta catalysts, *Macromolecules* **27** (1994) 7538-7543.
79. Leclerc, M. K., Brintzinger, H.-H., Zr-alkyl Isomerization in ansa-zirconocene-catalyzed olefin polymerizations. Contributions to stereoerror formation and chain termination, *J. Am. Chem. Soc.* **118** (1996) 9024-9032.

80. Busico, V., Caporaso, L., Cipullo, R., Landriani, L., Propene polymerization promoted by C₂-symmetric metallocene catalysts: From atactic to isotactic polypropene in consequence of an isotope effect, *J. Am. Chem. Soc.* **118** (1996) 2105-2106.
81. Busico, V., Cipullo, R., Influence of monomer concentration on the stereospecificity of 1-alkene polymerization promoted by C₂-symmetric ansa-metallocene catalysts, *J. Am. Chem. Soc.* **116** (1994) 9329-9330.
82. Resconi, L., Fait, A., Piemontesi, F., Colonna, M., Rychlicki, H., Zeigler, R., Effect of monomer concentration on propene polymerization with the rac-[Ethylenebis(1-indenyl)]zirconium dichloride / methylaluminoxane catalyst, *Macromolecules* **28** (1995) 6667-6676.
83. a) Izzo, L., Caporaso, L., Senatore, G., Oliva, L., Branched polyethylene by ethylene homopolymerization with meso-zirconocene catalyst, *Macromolecules* **32** (1999) 6913-6916. b) Izzo, L., Caporaso, L., Senatore, G., Oliva, L. *ibid.* 8695.
84. Izzo, L., De Riccardis, F., Alfano, C., Caporaso, L., Oliva, L., Formation of quaternary carbon centers in ethylene polymerization with meso-isopropylidenebis(1-indenyl)zirconium dichloride activated by MAO, *Macromolecules* **34** (2001) 2-4.
85. Yano, A., Hasegawa, S., Kaneko, T., Sone, M., Sato, M., Akimoto, A., Ethylene/1-hexene copolymerization with Ph₂C(Cp)(Flu)ZrCl₂ derivatives: correlation between ligand structure and copolymerization behavior at high temperature, *Macromol. Chem. Phys.* **200** (1999) 1542-1553.
86. Johnson, L. K., Killian, C. M., Brookhart, M., New Pd(II)- and Ni(II)-based catalysts for polymerization of ethylene and α -olefins, *J. Am. Chem. Soc.* **117** (1995) 6414-6415.
87. Mecking, S., Johnson, L. K., Wang, L., Brookhart, M., Mechanistic studies of the palladium-catalyzed copolymerization of ethylene and α -olefins with methyl acrylate, *J. Am. Chem. Soc.* **120** (1998) 888-899.
88. Galland, G. B., de Souza, R. F., Mauler, R. S., Nunes, F. F., ¹³C NMR determination of the composition of linear low-density polyethylene obtained with [η^3 -methallyl-nickel-diimine]PF₆ complex, *Macromolecules* **32** (1999) 1620-1625.
89. Thorshaug, K., Rytter, E., Ystenes, M., Pressure effects on termination mechanisms during ethene polymerization catalyzed by dicyclopentadienylzirconium dichloride / methylaluminoxane, *Macromol. Rapid. Commun.* **18** (1997) 715-722.
90. Thorshaug, K., Støvneng, J. A., Rytter, E., Ystenes, M., Termination, isomerization, and propagation reactions during ethene polymerization catalyzed by Cp₂Zr-R⁺ and Cp*₂Zr-R⁺. An experimental and theoretical investigation, *Macromolecules* **31** (1998) 7149-7165.
91. Lehmus, P., Kokko, E., Leino, R., Luttikhedde, H. J. G., Rieger, B., Seppälä, J. V., Chain end isomerization as a side reaction in metallocene-catalyzed ethylene and propylene polymerizations, *Macromolecules* **33** (2000) 8534-8540.
92. Prosenc, M.-H., Brintzinger, H.-H., Zirconium-alkyl isomerizations in zirconocene-catalyzed olefin polymerization: A density functional study, *Organometallics* **16** (1997) 3889-3894.
93. Karol, F. J., Kao, S.-C., Wasserman, E. P., Brady, R. C., Use of copolymerization studies with metallocene catalysts to probe the nature of the active sites, *New J. Chem.* **21** (1997) 797-805.

94. Dang, V. A., Yu, L.-C., Balboni, D., Dall'Occo, T., Resconi, L., Mercandelli, P., Moret, M., Sironi, A., Simple route to bis(3-indenyl)methanes and the synthesis, characterization, and polymerization performance of selected racemic-dichloro[methylenebis(Rn-1-indenyl)]- zirconium complexes, *Organometallics* **18** (1999) 3781-3791.
95. Busico, V., Cipullo, R., Caporaso, L., Angelini, G., Segre, A. L., C₂-symmetric ansa-metallocene catalysts for propene polymerization: Stereoselectivity and enantioselectivity, *J. Mol. Catal. A: Chem.* **128** (1998) 53-64.
96. Rieger, B., Jany, G., Fawzi, R., Steinmann, M., Unsymmetric ansa-zirconocene complexes with chiral ethylene bridges: Influence of bridge conformation and monomer concentration on the stereoselectivity of the propene polymerization reaction, *Organometallics* **13** (1994) 647-653.
97. Dietrich, U., Hackmann, M., Rieger, B., Klinga, M., Leskelä, M., Control of stereoerror formation with high activity "dual-side" zirconocene catalysts: A novel strategy to design the properties of thermoplastic elastic polypropenes, *J. Am. Chem. Soc.* **121** (1999) 4348-4355.
98. Guerra, G., Cavallo, L., Moscardi, G., Vacatello, M., Corradini, P., Back-skip of the growing chain at model complexes for the metallocene polymerization catalysis, *Macromolecules* **29** (1996) 4834-4845.
99. Blom, R., Dahl, I. M., On the sensitivity of metallocene catalysts toward molecular hydrogen during ethylene polymerization, *Macromol. Chem. Phys.* **200** (1999) 442-449.
100. Koivumäki, J., Fink, G., Seppälä, J. V., Copolymerization of ethene / 1-dodecene and ethene / 1-octadecene with the stereorigid zirconium catalyst systems iPr[FluCp]ZrCl₂ / MAO and Me₂Si[Ind]₂ZrCl₂ / MAO: Influence of the comonomer chain length, *Macromolecules* **27** (1994) 6254-6258.
101. Shiono, T., Moriki, Y., Soga, K., Copolymerization of poly(propylene) macromonomer and ethylene with metallocene catalysts, *Macromol. Symp.* **97** (1995) 161-170.
102. Shaffer, T. D., Canich, J. A. M., Squire, K. R., Metallocene-catalyzed copolymerization of ethylene and isobutylene to substantially alternating copolymers, *Macromolecules* **31** (1998) 5145-5147.
103. Krentsel, B. A., Kissin, Y. V., Kleiner, V. J., Stotskaya, L. L., *Polymers and copolymers of higher α -olefins*, Hanser Publishers, München 1997, 374 p.
104. Denger, C., Haase, U., Fink, G., Simultaneous oligomerization and polymerization of ethylene, *Makromol. Chem. Rapid Commun.* **12** (1991) 697-701.
105. Uozumi, T., Soga, K., Copolymerization of olefins with Kaminsky-Sinn-type catalysts, *Makromol. Chem.* **193** (1992) 823-831.
106. Galland, G. B., Quijada, P., Mauler, R. S., de Menezes, S. C., Determination of reactivity ratios for ethylene/ α -olefin copolymerization catalysed by the C₂H₄[Ind]₂ZrCl₂/methylaluminumoxane system, *Makromol. Rapid Commun.* **17** (1996) 607-613.
107. Suhm, J., Schneider, M. J., Mülhaupt, R., Influence of metallocene structure on ethene copolymerization with 1-butene and 1-octene, *J. Mol. Catal. A: Chem.* **128** (1998) 215-227.

108. Kaminsky, W., Engehausen, R., Zoumis, K., Spaleck, W., Rohrmann, J., Standardized polymerizations of ethylene and propene with bridged and unbridged metallocene derivatives: a comparison, *Makromol. Chem.* **193** (1992) 1643-1651.
109. Lehmus, P., Structure-property relations of some highly active ansa-metallocene catalysts in olefin polymerization – a polymerization study, *Acta Polytechnica Scandinavica*, Chemical Technology Series No 280, Espoo 2001, 56 pp.
110. Heiland, K., Kaminsky, W., Comparison of zirconocene and hafnocene catalysts for the polymerization of ethylene and 1-butene, *Makromol. Chem.* **193** (1992) 601-610.
111. Kaminsky, W., Schlobohm, M., Elastomers by atactic linkage of α -olefins using soluble Ziegler catalysts, *Makromol. Chem. Macromol. Symp.* **4** (1986) 103-118.
112. Kaminsky, W., Külper, K., Brintzinger, H.-H., Wild, F., Polymerisation von propen und buten mit einem chiralen Zirconocen und methylaluminoxan als cocatalysator, *Angew. Chem.* **97** (1985) 507-508.
113. Ewen, J. A., Mechanisms of stereochemical control in propylene polymerizations with soluble Group 4B metallocene/methylalumoxane catalysts, *J. Am. Chem. Soc.* **106** (1984) 6355-6364.
114. Chien, J. C. W., He, D., Olefin copolymerization with metallocene catalysts. I. Comparison of catalysts, *J. Polym. Sci. Part A: Polym. Chem.* **29** (1991) 1585-1593.
115. Lehmus, P., Härkki, O., Leino, R., Luttikhedde, H. J. G., Näsman, J. H., Seppälä, J. V., Copolymerization of ethene with 1-hexene or 1-hexadecene over ethylene, dimethylsilylene and 1,4butanediylysilylene bridged bis(indenyl) and bis(tetrahydroindenyl) zirconium dichlorides, *Macromol. Chem. Phys.* **199** (1999) 1965-1972.
116. Beck, S., Brintzinger, H.-H., Alkyl exchange between aluminum trialkyls and zirconocene dichloride complexes - a measure of electron densities at the Zr center, *Inorg. Chim. Acta* **270** (1998) 376-381.
117. Spaleck, W., Antberg, M., Rohrmann, J., Winter, A., Bachmann, B., Kiprof, P., Behm, J., Herrmann, W. A., High molecular weight polypropylene through specifically designed zirconocene catalysts, *Angew. Chem. Int. Ed. Engl.* **31** (1992) 1347-1350.
118. Spaleck, W., Küber, F., Winter, A., Rohrmann, J., Bachmann, B., Antberg, M., Dolle, V., Paulus, E. F., The influence of aromatic substituents on the polymerization behavior of bridged zirconocene catalysts, *Organometallics* **13** (1994) 954-963.
119. Stehling, U., Diebold, J., Kirsten, R., Röhl, w., Brintzinger, H.-H., Jüngling, S., Mülhaupt, R., Langhauser, F., *ansa*-Zirconocene polymerization catalysts with annelated ring ligands - effects on catalytic activity and polymer chain length, *Organometallics* **13** (1994) 964-970.
120. Schneider, M. J., Suhm, J., Mülhaupt, R., Prosenc, M.-H., Brintzinger, H.-H., Influence of indenyl ligand substitution pattern on metallocene-catalyzed ethene copolymerization with 1-octene, *Macromolecules* **30** (1997) 3164-3168.
121. Ekholm, P., Lehmus, P., Kokko, E., Haukka, M., Seppälä, J. V., Wilén, C.-E., Synthesis and characterization of a silyl substituted bis(indenyl)zirconium dichloride and comparison of its olefin polymerization behavior to a siloxy substituted analogue, *J. Polym. Sci. Part A: Polym. Chem.* **39** (2001) 127-133.

122. Ewen, J. A., Jones, R. L., Razavi, A., Ferrara, J. D., Syndiospecific propylene polymerizations with group 4 metallocenes, *J. Am. Chem. Soc.* **110** (1988) 6255-6256.
123. Herfert, N., Montag, P., Fink, G., Elementary processes in the Ziegler catalysis 7: Ethylene, α -olefin and norbornene copolymerization with the stereorigid catalyst systems $iPr[FluCp]ZrCl_2/MAO$ and $Me_2Si[Ind]ZrCl_2/MAO$, *Makromol. Chem.* **194** (1993) 3167-3182.
124. Stevens, J. C., Insite catalyst structure / activity relationships for olefin polymerization, *Proceedings MetCon '93*, Catalyst Consultants Inc., Houston TX, May 1993, pp. 157-170.
125. Woo, T. K., Fan, L., Ziegler, T., A density functional study of chain growing and chain terminating steps in olefin polymerization by metallocene and constrained geometry catalysts, *Organometallics* **13** (1994) 252-2261.
126. Soares, J. B. P., Hamielec, A. E., Bivariate chain length and long chain branching distribution for copolymerization of olefins and polyolefin chains containing terminal double bonds, *Macromol. Theory Simul.* **5** (1996) 547-572.
127. Soga, K., Yanagihara, H., Lee, D., Effect of monomer diffusion in the polymerization of olefins over Ziegler-Natta catalysts, *Makromol. Chem.* **190** (1989) 995-1006.
128. Herrmann, H.-F., Böhm, L. L., Particle forming process in slurry polymerization of ethylene with homogeneous metallocene catalysts, *Polymer Commun.* **32** (1991) 58-61.
129. Koivumäki, J., Seppälä, J. V., Observations on the synergistic effect of adding 1-butene to systems polymerized with $MgCl_2/TiCl_4$ and Cp_2ZrCl_2 catalysts, *Macromolecules* **27** (1994) 2008-2012.
130. Lahti, M., Koivumäki, J., Seppälä, J. V., Study on process parameters in metallocene polymerizations, I. Apparent viscosity and macro-scale mass transfer, *Angew. Makromol. Chem.* **236** (1996) 139-153.
131. Walter, P., Trinkle, S., Suhm, J., Mäder, D., Friedrich, C., Mülhaupt, R., Short and long chain branching of polyethylene prepared by means of ethene copolymerization with 1-eicosene using MAO activated $Me_2Si(Me_4Cp)(N^tBu)TiCl_2$, *Macromol. Chem. Phys.* **201** (2000) 604-612.
132. Mehta, A. K.; Speed, C. S.; Canich, J. A. M.; Baron, N.; Folie, B. J.; Sugawara, M.; Watanabe, A.; Welborn, H. C., Long-chain branched polymers and their production, *Int. Pat. Appl. WO 96/12744*, 2 May 1996.
133. Randall, J. C., A review of high resolution liquid ^{13}C carbon nuclear magnetic resonance characterizations of ethylene-based polymers, *J.M.S. - Rev. Macromol. Chem. Phys.* **C29** (1989) 201-317.
134. Scholte, Th. G., Characterisation of long-chain branching in polymers, In *Developments in polymer characterisation*, vol 4, ed. J. V. Dawkins, Applied Science Publishers, Great Britain 1983, pp. 1-37.
135. Mirabella, F. M. Jr., Wild, L., Determination of long-chain branching distributions in polyethylenes, in *Polymer characterization, physical property, spectroscopic and chromatographic methods*, ed. C.D. Craver and T. Provder, Advances in Chemistry Series, vol. 227, American Chemical Society, Washington, USA 1990, pp. 23-44.

136. McLeish, T. C. B., Milner, S. T., Entangled dynamics and melt flow of branched polymers, *Adv. Polym. Sci.* **143** (1999) 195-256.
137. Seppälä, J., Löfgren, B., Lehmus, P., Malmberg, A., Copolymerization properties of siloxy-substituted bis(indenyl)zirconocene catalysts: modified rheological behavior, *Macromol. Symp.* **173** (2001) 227-235.
138. García-Franco, C. A., Srinivas, S., Lohse, D. J., Brant, P., Similarities between gelation and long chain branching viscoelastic behavior, *Macromolecules* **34** (2001) 3115-3117.
139. Wang, W.-J., Yan, D., Charpentier, P. A., Zhu, S., Hamielec, A. E., Sayer, B. G., Long chain branching in ethylene polymerization using constrained geometry metallocene catalyst, *Macromol. Chem. Phys.* **199** (1998) 2409-2416.